Gaussian Beams

Enrique J. Galvez
Department of Physics and Astronomy
Colgate University

Contents

Chapter 1

Fundamental Gaussian Beams

In the last few decades the use of laser beams has become widespread. Lasers are used in both science and technology, from spectroscopical analysis to bar-code reading. It is therefore appropriate that we study the properties of laser beams in some detail. Laser beams of distinct types and colors have a few features in common: they are composed of a narrow band of wavelengths, to the point that we can call them "monochromatic" (*i.e.*, of a single wavelength), and they are collimated, that is, the light energy is restricted in the direction transverse to the propagation direction to form a narrow beam, as shown in Fig. 1.1 In a plane that is transverse to the propagation direction

Figure 1.1: A laser beam from a HeNe laser seen due to scattering.

the intensity of the beam decreases in a typical Gaussian shape. In this section we will discuss the basic properties of these (Gaussian) laser beams.

1.1 Spherical Wavefront in the Paraxial region

We will start by getting a rough idea of the mathematical representation of the light waves in Gaussian beams. Although we see that the beam is collimated, we also observe that the beam expands as it propagates.

We will use the z axis as the propagation direction of the laser beam, leaving the x and y directions for describing the transverse extension of the beam. The simplest

types of 3-D waves are plane waves. A plane wave propagating along the z direction is represented by the wave function

$$\Psi(x, y, z, t) = Ae^{i(kz-\omega t)}. \tag{1.1}$$

The amplitude A is constant. This equation cannot possibly describe a laser beam because the amplitude is infinitely extended in the transverse direction. A more appropriate amplitude would be one which decreases for points away from the z axis. We may "guess" something simple, like a Gaussian:

$$A = A(x, y) = e^{-(x^2+y^2)/w^2}, \tag{1.2}$$

where w is proportional to the width of the beam, also known as the beam spot. It is defined as the distance from the beam axis where the amplitude has decreased by $1/e$. Thus, the beam profile in Fig. 1.2a might be represented by the function in Fig. 1.2b. We note that the "intensity" of the beam shown in Fig. 1.2a is represented by the square of the amplitude, as we will see later in the course. The square of the Gaussian is another Gaussian with a width that is smaller by a factor of $\sqrt{2}$.

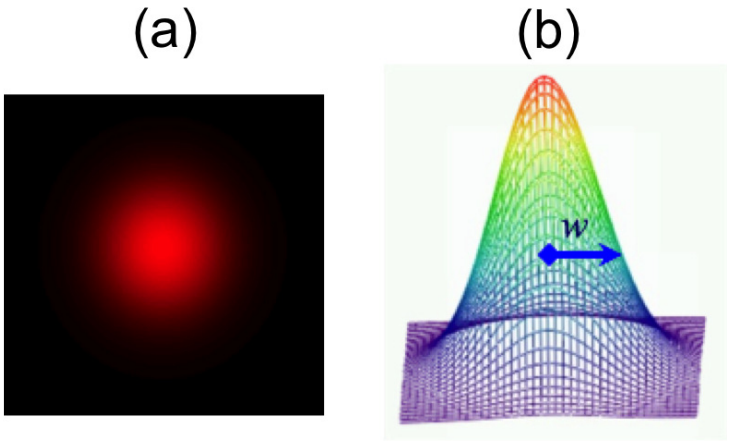

Figure 1.2: (a) False color image of the profile of a laser beam; (b) Profile of a Gaussian function in two dimensions.

The expansion of the beam may be accounted by a beam spot that increases with z, although the exact dependence is yet to be determined. If the beam is expanding then its "wavefront" must have a spherical shape. This is because a wave always propagates in a direction perpendicular to its wavefront (*e.g.*, ripples on a pond). The wavefront is defined as the surface that contains all points of the wave that carry the same phase (*e.g.*, the crest of the ripples). This spherical wavefront is

not accounted fully by the plane-wave phase term e^{ikz}, so we must use a modified expression.

The spatial part of a spherical wavefront has the form

$$e^{ikr}, \tag{1.3}$$

where

$$r = \sqrt{x^2 + y^2 + z^2}. \tag{1.4}$$

Let's suppose that we are examining the wave far from the origin but close to the z-axis such that $x \ll z$ and $y \ll z$. Then we can approximate Eq. 1.4 using the binomial approximation

$$r = z\sqrt{\frac{x^2 + y^2}{z^2} + 1} \simeq z\left(1 + \frac{x^2 + y^2}{2z^2}\right). \tag{1.5}$$

Thus a better approximation for the phase of the wave would include a phase similar to the one of a spherical wave. Our best guess for the expression of the wave function of the Gaussian beam may be

$$\Psi(x, y, z) \sim e^{-(x^2+y^2)/w^2} e^{i(kz-\omega t)} e^{ik(x^2+y^2)/2z}. \tag{1.6}$$

The first term contains the Gaussian profile, the second term has the unidirectional wave term, and the third term has the correction to the previous term that accounts for the curvature of the wavefront.

Exercise 1 Suppose that we have a HeNe laser beam with a wavelength of 632.8 nm. Consider the beam stopping on a piece of paper 2 m away from the laser. A that point the beam has a beam spot of about 3 mm. The profile is smooth and decreasing with an apparent Gaussian shape. However, the phase variation across this profile is that of a spherical wavefront, so that in the transverse plane the phase also increases. Find the distance $s = \sqrt{x^2 + y^2}$ from the center of the beam at which the phase has increased by 2π with respect to the center. Assume $z = 0$ is the center of the laser.

1.2 Formal Solution of the Wave Equation

Obviously the expression for the light from a laser beam cannot be guessed. We must get it by solving the wave equation. The three-dimensional wave equation is given by

$$\nabla^2\Psi - \frac{1}{v^2}\frac{\partial^2\Psi}{\partial t^2} = 0, \tag{1.7}$$

where

$$\nabla^2 = \frac{\partial}{\partial x^2} + \frac{\partial}{\partial y^2} + \frac{\partial}{\partial z^2}$$

is the Laplacian. If we introduce a trial solution of the form

$$\Psi(x, y, x, t) = U(x, y, z)e^{-i\omega t}. \tag{1.8}$$

Here U is the part of the wave function that depends only on the spatial coordinates. Replacing Eq 1.8 into Eq. 1.7 we get the *Helmholtz equation*:

$$\nabla^2 U + k^2 U = 0. \tag{1.9}$$

Note that we could have also chosen to use $e^{+i\omega t}$ in Eq. 1.8. In that case the solution would represent a wave that moves toward the negative z direction. Thus, the solution is *independent of the direction of propagation*.

Now we must simplify this equation given that we will restrict it to describe laser beams. We start by requiring that the solution must have the form

$$U(x, y, z) = U_0(x, y, z)e^{ikz}. \tag{1.10}$$

Replacing Eq. 1.10 into Eq. 1.9 and simplifying we get

$$\frac{\partial^2 U_0}{\partial x^2} + \frac{\partial^2 U_0}{\partial y^2} + \frac{\partial^2 U_0}{\partial z^2} + 2ik\frac{\partial U_0}{\partial z} = 0. \tag{1.11}$$

Exercise 2 Verify that replacing Eq. 1.10 into Eq. 1.9 results in Eq. 1.11.

The term e^{ikz} of Eq. 1.10 accounts for the wave oscillation along the propagation direction. The dependence of U_0 with z is of a different nature. It likely accounts for the slow decrease in the amplitude of the wave as the wave propagates. Thus we can say that U_0 varies *slowly* with z, and thus we can neglect the term $\partial^2 U_0/\partial z^2$ in front of the other ones and drop it from Eq. 1.11. The resulting equation

$$\frac{\partial^2 U_0}{\partial x^2} + \frac{\partial^2 U_0}{\partial y^2} + 2ik\frac{\partial U_0}{\partial z} = 0 \tag{1.12}$$

is called the *paraxial wave equation*.

A "simple" solution to the wave equation is one where we insert the simplest possible form of the solution and find the exact form that obeys the wave equation. The more formal solution is one where we just solve the wave equation in its full generality.

We "guess" the simple trial solution to be of the form

$$U_0(x,y,z) = Ae^{\frac{ik(x^2+y^2)}{2q(z)}}e^{ip(z)}. \tag{1.13}$$

Note how we separated the x, y and z dependencies. Upon replacing Eq. 1.13 into Eq. 1.12 we get separate equations for $q(z)$ and $p(z)$. Here we are not going to cover the step-by-step derivations. We will just show the solutions. For $q(z)$ we have that it is a complex function

$$q(z) = z - iz_R, \tag{1.14}$$

where z_R is a constant called the *Rayleigh range*. We will examine its significance later. Since $q(z)$ appears in the denominator of a fraction in the exponential of Eq. 1.13, then a more appropriate way to express it is by

$$\frac{1}{q(z)} = \frac{1}{z + \frac{z_R^2}{z}} + \frac{i}{\frac{z^2}{z_R} + z_R}. \tag{1.15}$$

Inserting Eq. 1.15 into the first exponential term of Eq. 1.13 we get

$$e^{\frac{ik(x^2+y^2)}{2R(z)}}e^{-\frac{x^2+y^2}{w(z)}}. \tag{1.16}$$

These terms have the form that we guessed in the first section. R(z) is known as the *radius of curvature of the wavefront*. It is given by

$$R(z) = z + \frac{z_R^2}{z} \tag{1.17}$$

For the second term of Eq. 1.16 we see that what we interpreted earlier as the beam spot of the beam has now a z-dependence

$$w(z) = w_0\sqrt{1 + \frac{z^2}{z_R^2}} \tag{1.18}$$

where the constant

$$w_0 = \sqrt{\frac{z_R\lambda}{\pi}} \tag{1.19}$$

is called the beam *waist*. Turning this equation around, we get an expression for the Rayleigh range:

$$z_R = \frac{\pi w_0^2}{\lambda}. \tag{1.20}$$

Before we analyze what all these terms mean let's look at the solution for $p(z)$:

$$e^{ip(z)} = \frac{w_0}{w(z)}e^{-i\varphi(z)}, \tag{1.21}$$

where

$$\varphi(z) = \arctan(z/z_R) \tag{1.22}$$

is known as the *Gouy phase*.

Now let's put it all together:

$$\Psi(x,y,z,t) = A\frac{w_0}{w(z)} e^{-\frac{x^2+y^2}{w(z)^2}} e^{i(kz-\omega t)} e^{\frac{ik(x^2+y^2)}{2R(z)}} e^{-i\varphi(z)} \tag{1.23}$$

The first three terms specify the amplitude of the wave, and the next three terms define the phase of the wave embedded in the exponential terms. Now let's analyze the meaning of all of these terms.

1.2.1 Beam Spot $w(z)$

Consider Eq. 1.18. The function $w(z)$ represents the beam spot of the beam. Figure 1.3 shows a graph of $w(z)$. Note the two limits for z:

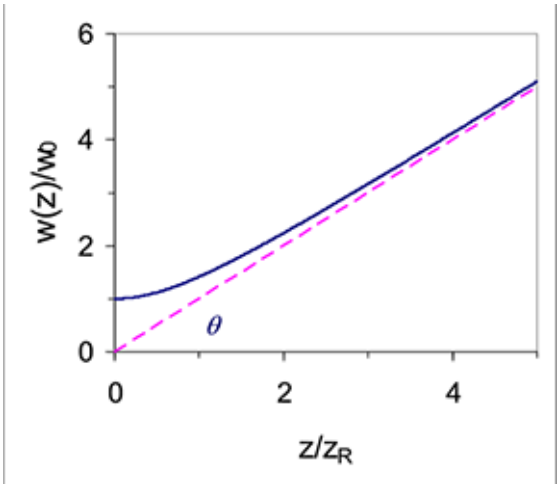

Figure 1.3: Graph of the beam spot of the beam.

- When $z = 0$ we have $w(z) = w_0$. Notice that this the smallest value that $w(z)$ can have. Thus $z = 0$ is a special point in the propagation of the beam. For $z > 0$ the beam spot increases. In the negative z direction the beam spot also increases. Thus, Fig 1.3 describes the width of a beam when it is focused by a lens. When a light beam is focused there is always a minimum width of the beam at the focal point. This minimum beam spot can be understood in terms of diffraction.

- When $z = z_R$ we have $w(z) = \sqrt{2}w_0$. This is a turning point in the propagation of the light as the beam spot makes the transition from being nearly constant to increasing linearly (dashed line in Fig. 1.3). When $z < z_R$ the ray description of the propagation of the light breaks down. It is important to note that the Raleigh range is an indicator of the divergence of the beam: the smaller the value of z_R the quicker it will turn to expand linearly. The confocal parameter is defined $2z_R$. It is important for many problems in Gaussian-beam optics because it refers to the distance over which the beam diameter in nearly constant. The radius of curvature of the beam at $z = z_R$ is $R = 2z_R$. Confocal laser resonators have a radius of curvature equal to their separation d, or $d = 2z_R$.

- When $z \gg z_R$ the beam spot expands linearly as $w(z) = w_0 z/z_R = z\theta$ (*i.e.,* approaching the dashed lines in Fig 1.3). At this limiting value θ is called the divergence angle of the beam

$$\theta = \frac{\lambda}{\pi w_0}. \tag{1.24}$$

Note that the smaller the waist the larger the divergence angle. It is interesting that we get a similar result out of diffraction of light from a small aperture. If the aperture is a slit the equation for the first minimum of diffraction is

$$b \sin\theta = \lambda,$$

where b is the width of the slit. For small angles we can approximate this relation to

$$\theta = \frac{\lambda}{b}.$$

For a circular aperture $2a$, where a is the radius of the aperture, the angle at which the first diffraction minimum appears is given by

$$\theta = \frac{1.22\lambda}{2a}.$$

You can see that aside from a constant factor the expressions for diffraction angle are the same as that of the divergence of the beam. The reason *is* the same one. If we had an opaque piece of glass with a transparent circular region with a transparence that varies like a Gaussian, we will get a divergence angle that is given indeed by Eq. 1.24.

In ordinary situations we have the following relation to hold

$$\lambda \ll w_0 \ll z_R. \tag{1.25}$$

Let's do a numerical example. Suppose that we have a HeNe laser beam (λ =632.8 nm) that is focused to a spot $w_0 = 0.5$ mm. The Raleigh range is $z_R = \pi w_0^2/\lambda = 1.2$ m.

Exercise 3 Another important aspect related to the Gaussian waist is the amount of light that passes through a circular aperture. The intensity of the light at a given radius a is given by

$$I = I_0 e^{-2a^2/w^2}.$$

1. Show that the fraction of the total power that gets transmitted through a circular aperture of radius a_0 is

$$P(a) = 1 - \exp(-2a_0^2/w^2). \tag{1.26}$$

2. Calculate the percentage of light that goes through an aperture of radius $a_0 = w$

1.2.2 Beam Amplitude

The dependence of the amplitude with z is given by $w_0/w(z)$. From the analysis of $w(z)$ in the previous section we gather that for $z < z_R$ the amplitude is nearly constant, but for $z \gg z_R$ it decreases as $1/z$. The decrease of amplitude with z at large values of z leads us to conclude that in this limit the amplitude varies like the amplitude of a spherical wave (*i.e.,* $\propto 1/r$).

1.2.3 Wavefront

As seen in Eq. 1.23 there are three phase terms. The first and third phases, $(kz - \omega t)$ and ϕ depend only on z. The middle term contains the phase $k(x^2 + y^2)/2R(z)$. From the discussion in section 1.1 we interpreted the latter term as representing the curvature of the wavefront. The wavefront is spherical with a radius of curvature $R(z)$. What is interesting is that the radius of curvature is not constant. Figure 1.4 shows sketchings of the wavefronts at different values of z. Notice first that when we graph the beam spot of the beam into the negative values of z the beam spot increases in the same way that it does in the positive z direction. The thinner curves are sketches of the wavefronts with radii of curvature given by Eq. 1.17. Let's consider the limits, but for this let's rewrite $R(z)$ as

$$R(z) = z(1 + \frac{z_R^2}{z^2}). \tag{1.27}$$

- When $z = 0$ we have $R = \infty$ (a vertical line in Fig. 1.4). It is the phase that we would expect of a plane wave. At this point all parts of the wave are moving in the same direction.

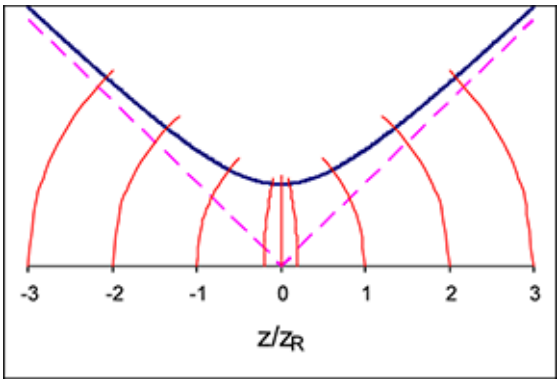

Figure 1.4: Graph of the beam spot of the beam showing the shape of the wavefronts.

- When $z \gg z_R$ then $R(z) \simeq z$; the wavefront is a spherical surface traveling away from $z = 0$. This is the geometric optics limit. When we focus a beam of light we expect the light "rays" to go in straight lines to and from the focal point ($z = 0$). This is correct as long as $|z| \gg z_R$. For $|z| < z_R$ the wave aspect of the light manifests. Otherwise the ray-optics view would predict that the focal point is a singularity.
- When $z = z_R$ then $R(z) = 2z$; the turning point between ray-optics and wave-optics.

1.2.4 Gouy Phase

There is an intriguing phase term in Eq. 1.23: the Gouy phase, given explicitly by Eq 1.22. This phase slightly shifts the phase of the wavefront of the wave as a whole. If we picture a wave being focused like that in Fig. 1.4 the Gouy phase varies as shown in Fig. 1.5.

As $z \to \pm\infty$ the Gouy phase asymptotes to $\phi(z) \to \pm\pi/2$. Thus the phase shift from $z = -\infty$ to $z = \infty$ is only π. Notice that all of the action occurs between $z = -z_R$ and $z = z_R$.

The Gouy phase is relevant only in situations where the wavefront is very complex. We will not consider it further here.

1.3 Focusing a Gaussian Beam

We must now consider the effect of a lens on a Gaussian wavefront. We have not discussed yet the physics behind lenses, but you may have seen some of it in a past course. In any of those contexts you may have seen a "lens equation" that describes

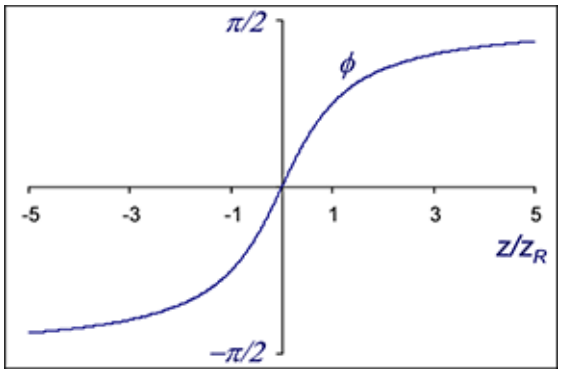

Figure 1.5: Graph of the Gouy phase $\varphi(z)$.

a relation between the focal length of a lens and the locations of an object and the image that the lens forms of that object. Here we will treat lenses differently. We will treat them "locally." That is, as a device that modifies the radius of curvature of a spherical wavefront, as shown in Fig. 1.6.

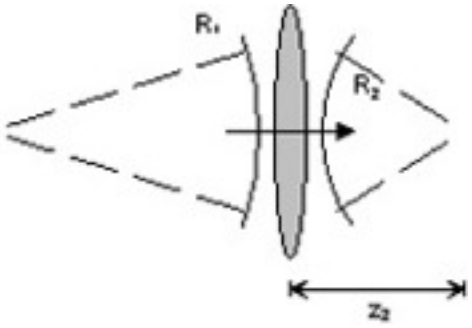

Figure 1.6: Change in the radius of cuvature of the wavefront by passage through a lens.

If the beam that is incident on a lens of focal length f has a radius of curvature R_1 then the radius of curvature of the outgoing wave R_2 is given by

$$\frac{1}{R_2} = \frac{1}{R_1} - \frac{1}{f}. \tag{1.28}$$

It is important to note that there is a sign convention: the radius is positive when the center curvature is to the left. In Fig. 1.6 $R_1 > 0$ and $R_2 < 0$. The typical cases of ray optics have similar correspondence with the wave optics form of Eq. 1.28 (the wave optics limit fully agrees with the ray optics in the limit that $\lambda \to 0$). For example, if the input beam is fully collimated ($R_1 = \infty$) then $R_2 = -f$, or if $R_1 = f$ then $R_2 = \infty$.

Once we know the radius of curvature of the beam past the lens we then want to know the place where the minimum beam spot is going to be located and the size of the waist. The waist location is given by[1]

$$z_2 = \frac{R_2}{1 + \left(\frac{R_2}{\pi w_2^2/\lambda}\right)^2}, \tag{1.29}$$

where w_2 is the beam spot of the beam just after the lens, which is the same as the beam spot just before the lens w_1 (*i.e.*, $w_2 = w_1$). Notice that under "ordinary" situations

$$R_2 \ll \pi w_2^2/\lambda. \tag{1.30}$$

For example. If a beam with a beam spot $w_1 = 1$ mm is incident on a lens that changes its radius to say $R_2 = 10$ cm, then we see that $\pi w_2^2/\lambda = 5$ m, consistent with Eq. 1.30. When Eq 1.30 holds Eq. 1.29 becomes

$$z_2 \simeq R_2. \tag{1.31}$$

This is the geometric optics limit. The waist is given by

$$w_{02} = \frac{w_2}{\left[1 + \left(\frac{\pi w_2^2/\lambda}{R_2}\right)^2\right]^{1/2}}. \tag{1.32}$$

Notice that for the "ordinary" situations that we mentioned (*i.e.*, Eq. 1.30) the waist reduces to

$$w_{02} \simeq \frac{\lambda R_2}{\pi w_2}. \tag{1.33}$$

In many situations we have reasons to focus the light to the smallest spot. For example, in laser welding you need the highest radiant energy in the smallest spot so that you can get enough energy to melt metal. Another reason to focus the light into the smallest spot stems from the need to send light to a small object but not to its neighbors. From Eq. 1.33 se see that to get a small waist one needs:

1. A small value R_2, which implies a lens with a small focal length f,
2. the smallest possible wavelength, and
3. a large beam spot w_2 of the beam at the lens.

Equation 1.33 can be put in a different form. If we use a lens with a focal length f and diameter d, then it has an f-number $f\# = f/d$. If the incoming beam with $R_1 \gg f$ fills the lens then $R_2 \sim f$ and $w_2 \sim d/2$, so Eq. 1.33 reduces to $w_{02} \sim 2\lambda f\#/\pi$. This implies that in order to focus the beam to a small spot one needs a lens with a small $f\#$.

[1]F.L. Pedrotti and L.S. Pedrotti in *Introduction to Optics* (Prentice Hall, 1993) p. 461

1.4 Problems

Problem 1 Consider the plane wave traveling in free space where $k = 2\pi(1,1,1)/(\lambda\sqrt{3})$, where $\lambda = 600$ nm, and with an electric field amplitude of 10 V/m. The phase of the wave is 2π at the origin.

1. Find an expression for the wave using the complex notation.
2. Find the frequency f of the wave in THz.
3. Find a point other than the origin where the phase is 2π at $t = 0$.

Problem 2 A beam from a HeNe laser ($\lambda = 632.8$ nm) is traveling along the z-axis and has a waist $w_0 = 0.1$ mm at $z = 0$.

1. What is the beam spot at $z = 10$ cm?

   Ans. $z_R = 0.05$ m, $w = 0.0224$ cm
2. What is the radius of curvature of the wave front R at $z = 10$ cm?

   Ans. $R = 12.5$ cm
3. At what distance z_1 is $R = 2$ m?

   Ans. $z_1 \geq 2$ m
4. Make a graph of R/z *vs.* z from $z = 0$ to $z = 1$ m.

   Ans. Infinite at $z = 0$ coming down to an asymprote at $R/z = 1$ for $z \gg z_R$
5. Explain the shape of the curve for part (4).

   Ans. At $z = 0$ $R = \infty$; but as $z \gg z_R$, $R \sim z$
6. Make a graph of w *vs.* z from $z = 0$ to $z = 0.5$ m.

   Ans. $w = w_0$ at $z = 0$, curving up to $w \sim z$ for $z \gg z_R$
7. Comment of the shape of the previous graph and explain its significance.

   Ans. As $z \gg z_R$, $w \sim z$
8. Assuming that the phase of the wave is 2π at $z = 0$ and $t = 0$, find the phase of the wave (modulo 2π) at $z = 0.1$ m (and $t = 0$). [If $\phi = 6.1\pi$, $\phi(\text{mod}2) = 6.1\pi - 3(2\pi) = 0.1\pi$.]

   Ans. $\phi = 5.1\text{rad} = 1.6\pi$

9. Find the phase of the wave (modulo 2π) at $z = z_R$, $x = w(z = z_R)$, $y = 0$ (and $t = 0$).

   Ans. $\phi = 0.38$ rad

Problem 3 A laser beam has $\lambda = 670$ nm and $P = 3$ mW. The beam spot of the beam reaching a lens is 2 mm. The lens has a focal length $f_1 = 1$ cm.

1. If the radius of curvature of the wavefront reaching the lens is 2 m, find the waist of the focused light after the lens.

   Ans. $R_2 = 1.005$ cm, $w_{02} = 1.07 \cdot 10^{-6}$ m (using Eq. 1.33).

2. The intensity of the light at the center of a gaussian beam is given by $I_{\max} = 2P/\pi w_0^2$ (in W/m^2). Calculate the maximum intensity at the focal point.

   Ans $I_{\max} = 1.66 \cdot 10^9$ W/m^2

3. If we place a second lens with $f_1 = 10$ cm after the first one at a distance $d = f_1 + f_2$.

   (a) Calculate the beam spot of the beam at the second lens.
   Ans. $w_3 = 5.57 \cdot 10^{-6}$ m, $w(10\text{cm}) = 1.99$ cm.

   (b) What application do you see for this system of lenses?
   Ans. $w_3/w_2 \simeq 10$: Beam expander

Problem 4 A Gaussian beam of wavelength 600 nm and power 100 mW travels along the z-axis. It has a waist w_0 located at $z = 0$. At $z_1 = 32$ cm there is a lens with a focal length $f = 30$ cm. The beam spot at the lens is $w_1 = 6.1$ mm. After the lens there is a new waist w_{02}. After this waist is an iris of radius $r_i = 0.5$ mm, as shown in the figure. The iris is at a distance of 5 m from the lens.

1. Find the initial waist of the beam w_0.

2. Find the Rayleigh range z_{R2} of the light at the waist after the lens.

3. Find the beam spot of the beam w_3 at the iris. (Note that for the purpose of using the formulas you can treat each waist as a place where $z = 0$.)

4. What is the phase of the wave at the edge of the iris relative to the phase at the center of the iris?

5. What is the intensity of the beam at the edge of the iris?

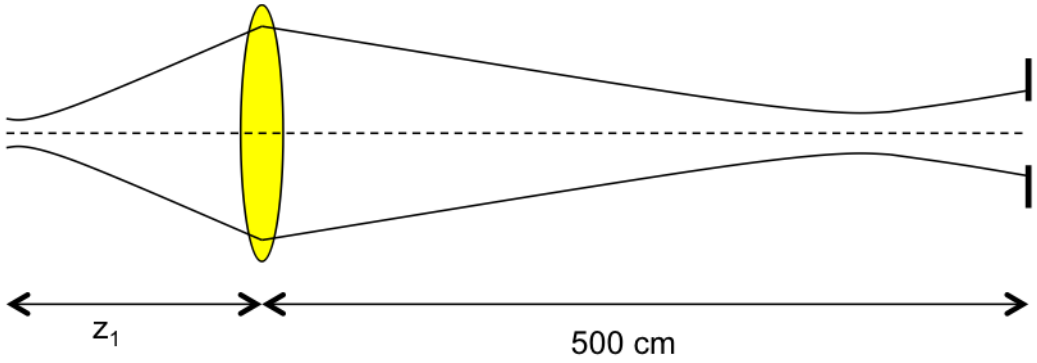
z1
500 cm

Chapter 2

High-Order Gaussian Beams

2.1 High-Order Gaussian Beams in Rectangular Coordinates

If you recall, in Chapter 2 we solved the paraxial wave equation by introducing a "guess" solution. The solution was not the most general because it defined the x and y dependencies in Eq. 2.13. That dependence did not allow differences in the x and y solutions. It then led to the simplest solution, Eq. 2.22. A more general trial solution may be given by

$$U_0(x,y,z) = Ag(x,z)h(y,z)e^{ik(x^2+y^2)/[2q(z)]}e^{ip(z)}. \tag{2.1}$$

By replacing this solution into the paraxial wave equation we get solution for g and h in terms of Hermite polynomials. The final solution is

$$U_{m,n}(x,y,z) = \frac{A}{w(z)}H_m(\frac{\sqrt{2}x}{w(z)})H_n(\frac{\sqrt{2}y}{w(z)})e^{-(x^2+y^2)/w(z)^2}e^{ik(x^2+y^2)/[2R(z)]}e^{-i\varphi(z)}. \tag{2.2}$$

The beam described by this solution is known as a Hermite-Gauss beam. The indices m and n of the Hermite polynomials provide a family of solutions. We define the order of the solution by $N = n + m$. Modes of the same order are degenerate in laser resonators. The lowest-order Hermite polynomials $\mathrm{H}_m(v)$ are

$$\mathrm{H}_0(v) = 1 \tag{2.3}$$
$$\mathrm{H}_1(v) = 2v \tag{2.4}$$
$$\mathrm{H}_2(v) = 4v^2 - 2 \tag{2.5}$$

From Eq. 2.3 we can conclude that the solution of Gaussian beams discussed earlier (Eq. 2.22) is only the zero-order ($N = 0$) solution of Eq. 2.2.

Figures 2.1 (a) and (b) show graphs of the amplitude of the HG_{10} and HG_{20} modes, respectively. To the right of the graphs are pictures of the corresponding laser-beam modes.

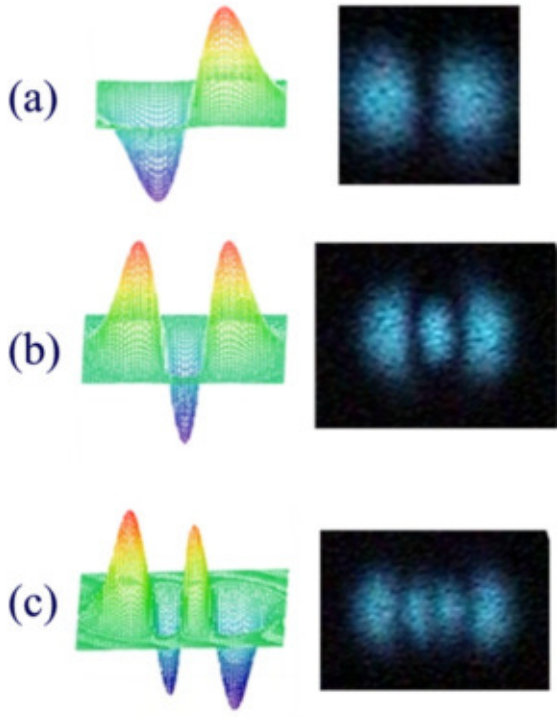

Figure 2.1: Graphs of the amplitude and pictures of Hermite-Gauss modes: (a)HG_{10}, (b) HG_{20}, (c) HG_{30}.

Exercise 4 Consider the amplitude of the general solution of the wave equation in rectangular coordinates, Eq. 2.2, at $z = z_0$, and with $x_0 = y_0 = w(z_0)$. Make sketches of

1. $U_{00}(x, 0, z_0)$ *vs.* x and $U_{00}(0, y, z_0)$ *vs.* y.

   Ans. A Gaussian for both graphs.

2. $U_{01}(x, y_0, z_0)$ *vs.* x and $U_{01}(0, y, z_0)$ *vs.* y.

   Ans. The mode is similar to Fig. 2.1 (a) but rotated 90 degrees, so graph vs. x is a Gaussian, but vs. y goes as a horisontal cut of Fig. 2.1(a).

3. $U_{02}(x, y_0, z_0)$ *vs.* x and $U_{02}(0, y, z_0)$ *vs.* y.

Ans. The mode is similar to Fig. 2.1 (b) but rotated 90 degrees, so graph vs. x is a Gaussian, but vs. y goes as a horisontal cut of Fig. 2.1(b).

4. $U_{11}(x, y_0, z_0)$ *vs.* x and $U_{11}(x_0, y, z_0)$ *vs.* y, where $x_0 = y_0 = w(z_0)$.

   Ans. The mode is similar to Fig. 2.6 (four lobes) but squared with the axes, so graph vs. x is a and graph vs. y look the same as U_{01}vs.y.

Draw a rough shape of the beam profiles for each of the cases above.

Ans. Mentioned above.

Aside from the Hermite polynomials, the other terms of Eq. 2.2 are the same as those in Eq. 1.23 except for the Gouy phase, which in Eq. 2.2 has a new factor: $\varphi(z) = (N+1)\tan^{-1}(z/z_R)$. The constant term in Eq. 2.2 that normalizes the square of the amplitude is given by

$$A = \left(\frac{2^{1-N}}{\pi n!m!}\right)^{1/2}. \tag{2.6}$$

This gives

$$A = \sqrt{\frac{2}{\pi}} \tag{2.7}$$

for $N = 0$.

One can understand these modes with the analogy of a drum. The membrane of the drum can oscillate in its lowest-order mode: the whole membrane goes up an down. This mode has the lowest pitch. The next higher-order mode is one where the two halves of the membrane oscillate 180 degrees out of phase. This oscillation will have a higher pitch. There is a node along the middle of the membrane. This would be mode 01. A mode with a node orthogonal to it would be the mode 10. Notice that the placing of the node is arbitrary. Thus, modes 01 and 10 are "degenerate;" they oscillate at the same frequency. You can also imagine other higher-order solutions. All in analogy to the modes of the light.

2.2 High-Order Gaussian Beams in Cylindrical Coordinates

The physics of high-order modes gets much more interesting with the solutions of the paraxial equation in cylindrical coordinates. The relations between the cylindrical and Cartesian coordinates are:

$$r = \sqrt{x^2 + y^2} \tag{2.8}$$

$$\theta = \tan^{-1}(y/x) \tag{2.9}$$

$$z = z \tag{2.10}$$

We will not do any derivations because they are outside the scope of the discussion. Suffices to state the solution, given by

$$U_{p,\ell}(r,\theta,z) = \frac{A}{w(z)}\left(\frac{\sqrt{2}r}{w(z)}\right)^{|\ell|} L_p^{|\ell|}\left(\frac{2r^2}{w(z)^2}\right) e^{-r^2/w(z)^2} e^{ikr^2/[2R(z)]} e^{i\ell\theta} e^{-i\varphi(z)}. \quad (2.11)$$

The solution now contains the associated Laguerre function L_p^ℓ, and reason for calling these modes Laguerre-Gauss. The subindices p and ℓ now account for the families of solutions of order $N = 2p + |\ell|$. The constant term in Eq. 2.11 that normalizes the solution is given by

$$A = p!\left(\frac{2}{\pi p!(|\ell| + p)!}\right)^{1/2}. \quad (2.12)$$

Notice that for $N = 0$ we aso get Eq. 2.7.

One of the main characteristics of the solution is that the amplitude has a pure radial dependence, so that the intensity profile of the beams consists of one or more rings, as shown in Fig. 2.2. When $\ell \neq 0$ and $p = 0$ the beams have a characteristic single-ringed "doughnut," with the radius of the doughnut proportional to $\ell^{1/2}$.

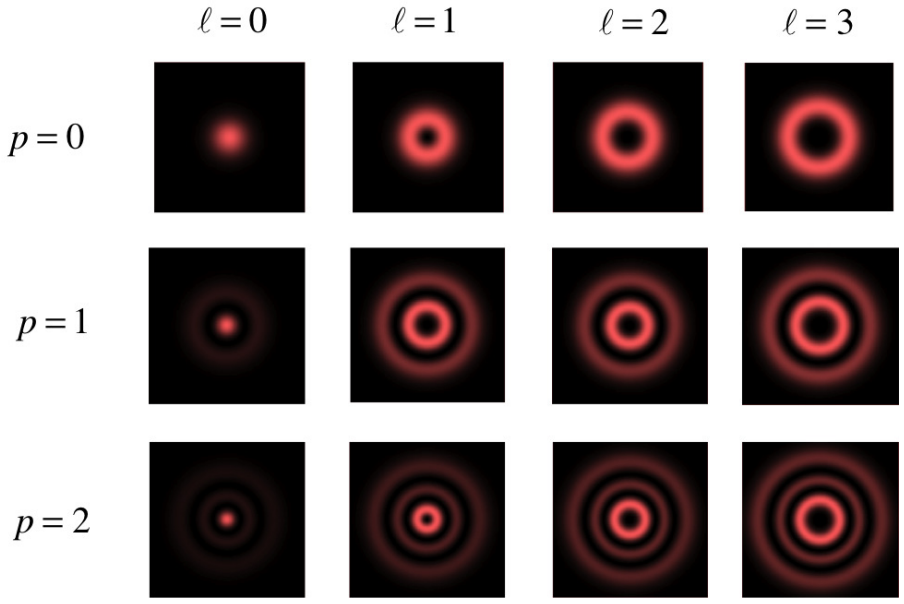

Figure 2.2: Graph of the amplitude of lowest-order Laguerre-Gauss modes.

Exercise 5 The expression for the amplitude of an LG mode is

$$U_{p,\ell}(r,\theta,z) \propto \left(\frac{\sqrt{2}r}{\omega_0}\right)^{|\ell|} \mathrm{L}_p^{|\ell|}\left(\frac{2r^2}{\omega(z_0)^2}\right) \exp\left[\frac{-r^2}{\omega(z)^2}\right], \quad (2.13)$$

where $\mathrm{L}_p^{|\ell|}(v)$ is the associated Laguerre polynomial of radial order p and azimuthal order ℓ. The first three polynomials are:

$$\mathrm{L}_0^{|\ell|}(v) = 1 \tag{2.14}$$

$$\mathrm{L}_1^{|\ell|}(v) = 1 + |\ell| - v \tag{2.15}$$

$$\mathrm{L}_2^{|\ell|}(v) = \frac{1}{2}\left[v^2 - 2(|\ell| + 2) + (|\ell| + 1)(|\ell| + 2)\right] \tag{2.16}$$

Make sketches of:

1. $U_{00}(r, \theta, z_0)$ *vs.* r

   Ans. A Gaussian (round beam mode).

2. $U_{02}(r, \theta, z_0)$ *vs.* r

   Ans. A cut to to Fig. 2.2 ($p = 0$, $\ell = 2$).

3. $U_{10}(r, \theta, z_0)$ *vs.* r

   Ans. A cut to to Fig. 2.2 ($p = 1$, $\ell = 0$).

4. Draw a rough shape of the beam profiles for each of the cases above.

   Ans. In Fig. 2.2.

Returning to the full solution Eq. 2.11, the most interesting term is the one where the phase varies as $\ell\theta$. That is, the phase of the wave depends on the angular coordinate, and winds in multiples (ℓ) of 2π when we go one revolution about the center of the beam. This can be seen in Fig. 2.3, where we show the color coded phase instead of amplitude.

Ignoring for the moment the correction due to the radius of curvature of the phase front (or equivalently assuming $R(z) \to \infty$), we find that the phase of the wave has the form

$$\psi(r, \theta, z) = kz + \ell\theta. \tag{2.17}$$

Points of constant phase (i.e., the wave front) form a helix of pitch λ, as shown in Fig. 2.4 for the case $\ell = 1$. For $\ell > 1$ the wavefront consists of multiple helices. In a given transverse plane the phase depends on $\ell\theta$, as shown in Fig. 2.5. At $r = 0$ the phase is undefined; it is said to be a phase singularity, or optical vortex. For this reason the amplitude of the wave is zero at $r = 0$.

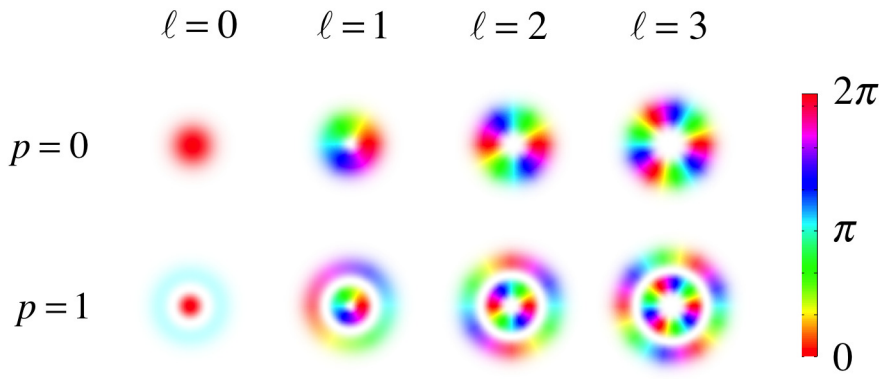

Figure 2.3: Images of the lowest-order Laguerre-Gauss modes, with the intensity color-coded with the phase of the wave at that point (see color legend).

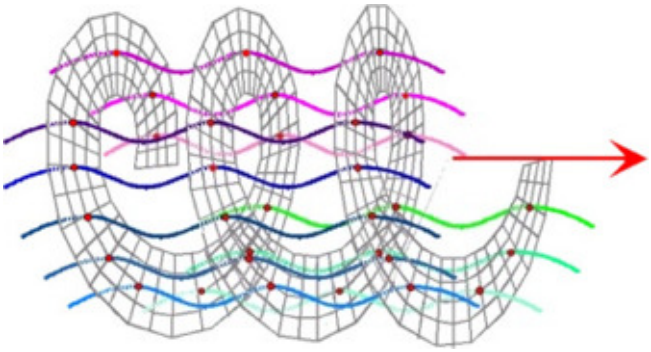

Figure 2.4: Graph of the wavefront of a LG_0^1 mode.

2.3 Relations Between Mode Families

Hermite-Gauss and Laguerre-Gauss modes are complete sets of functions. Any Spatial distribution can be expressed in terms of superpositions of them, and each solution in a given family can be expressed as a superposition of functions in the other family. The first-order modes of both families form an interesting case that we describe next.

The first-order Laguerre-Gauss modes can be expressed by

$$LG_0^\ell = A_1 r e^{i\ell\theta}\, G\, W, \tag{2.18}$$

where one mode has $\ell = +1$ and the other $\ell = -1$; A_1 is a constant given by

$$A_1 = \frac{2}{\sqrt{\pi} w^2}; \tag{2.19}$$

G is the Gaussian envelope

$$G = e^{-r^2/w^2}; \tag{2.20}$$

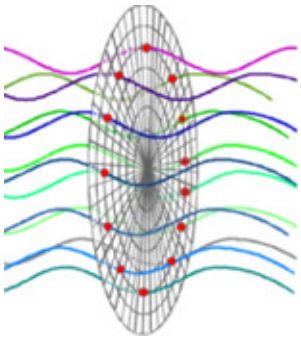

Figure 2.5: Graph of phase of a LG_0^1 mode across a transverse plane.

and W is the overall phase term,

$$W = e^{-ikr^2/(2R)-i\varphi}, \tag{2.21}$$

which includes the Gouy phase φ. As seen before, there are two first-order Hermite-Gauss modes. They are given by

$$HG_{10} = B_1 x\ G\ W \tag{2.22}$$

and

$$HG_{01} = B_1 y\ G\ W, \tag{2.23}$$

where we have combined the constants into the coefficient

$$B_1 = \frac{2\sqrt{2}}{\sqrt{\pi} w^2}. \tag{2.24}$$

Notice that $A_1 = B_1/\sqrt{2}$.

Using the Euler identity with Eq. 2.18 gives

$$LG_0^{\pm 1} = A_1(x \pm iy)\ G\ W \tag{2.25}$$

or equivalently,

$$LG_0^{\pm 1} = \frac{1}{\sqrt{2}}(HG_{10} \pm iHG_{01}), \tag{2.26}$$

which puts the two first-order Laguerre-Gauss modes in terms of the two first-order Hermite-Gauss modes. Furthermore, if a coordinate frame (x', y') is rotated from the (x, y) frame by an angle θ, then the mode HG_{10} rotated by an angle θ is

$$\begin{aligned} HG_{10}(\theta) &= B_1 x'\ G\ W \\ &= B_1 r\cos(\phi - \theta)\ G\ W \\ &= HG_{10}\cos\theta + HG_{01}\sin\theta, \end{aligned} \tag{2.27}$$

where the primed coordinates refer to those in the rotated reference frame: $x' = r\cos\phi' = r\cos(\phi - \theta)$. Manipulating Eq. 2.27 yields

$$\begin{aligned} HG_{10}(\theta) &= \frac{A_1}{\sqrt{2}} r(e^{i(\phi-\theta)} + e^{-i(\phi-\theta)})\; G\; W \\ &= \frac{1}{\sqrt{2}}(LG_0^{+1}e^{-i\theta} + LG_0^{-1}e^{i\theta}). \end{aligned} \tag{2.28}$$

This way we get the two first-order Hermine-Gauss modes in terms of the two first-order Laguerre-Gauss modes:

$$HG_{10} = \frac{1}{\sqrt{2}}(LG_0^{+1} + LG_0^{-1}) \tag{2.29}$$

$$HG_{01} = \frac{-i}{\sqrt{2}}(LG_0^{+1} - LG_0^{-1}). \tag{2.30}$$

These relations between families can be extended to higher orders. Also note that the zero orders are the same: $LG_0^0 = HG_{00}$

2.4 Irradiance and Power

In the section on electromagnetic waves we saw that the irradiance, or the time average flow of energy per unit time per unit area ($\mathrm{W/m^2}$), of a **plane** electromagnetic wave is given by

$$I = \frac{c\epsilon_0}{2} E_0^2, \tag{2.31}$$

where E_0 is the amplitude of the electric field of the wave. For Gaussian beams the amplitude of the electric field of the wave at any point is the value calculated earlier, U. However, U is normalized. The electric field of a beam of power P is

$$E = U\sqrt{\frac{2P}{c\epsilon_0}}. \tag{2.32}$$

For example, the amplitude of the field for the $N = 0$ beam is

$$U_0 = \sqrt{\frac{2}{\pi}}\frac{1}{w} e^{-r^2/w^2}, \tag{2.33}$$

where w is the half-width of the beam defined in Eq. 2.18, which varies with z. The irradiance of the beam then becomes

$$I = \frac{2P}{\pi w^2} e^{-2r^2/w^2}. \tag{2.34}$$

If we integrate the irradiance, we get the power

$$P = \int_0^\infty I \; 2\pi r dr \tag{2.35}$$

An important quantity in many fields is the maximum irradiance

$$I_{\max} = \frac{2P}{\pi w^2}. \tag{2.36}$$

For example, by focusing a 5-mW HeNe laser beam to a waist of 25 μm we get that $I_{\max} = 5$ MW/m^2. From the maximum irradiance we can get a value for the peak electric field of the wave:

$$E_{\max} = \sqrt{\frac{2I_{\max}}{c\epsilon_0}} = \frac{2}{w}\sqrt{\frac{P}{\pi c\epsilon_0}}. \tag{2.37}$$

The maximum electrc field for the previous example is 62 kV/m.

2.5 Problems

Problem 5 Light waves with a transverse profile described by Hermite-Gauss functions (or modes) of indices (m, n) are normally labeled as HG_{mn}. Make a sketch of the amplitude of the HG_{21}.

Problem 6 Light waves with a transverse profile described by Laguerre-Gauss functions (or modes) of indices (p, l) are normally labeled as LG_p^ℓ.

1. Show that the radius of the LG_0^l "doughnut" beam profile increases with $\ell^{1/2}$. The Fig. 2.6 shows a diffraction pattern where the zero order is the LG_0^0 and the patterns on each side are the LG_0^l modes, with $p = 0$ and increasing value of ℓ. Note: $L_0^l(v) = 1$.

   Ans. Differentiate $U_{p,l}$ with respect to r and equate to sero (maximum of the ring). Solve for r.

2. Using the analytical expression for the LG_p^ℓ modes, show that the modes with $\ell \neq 0$ have an amplitude of zero at the center.

   Ans. Depend on $r^{|\ell|}$.

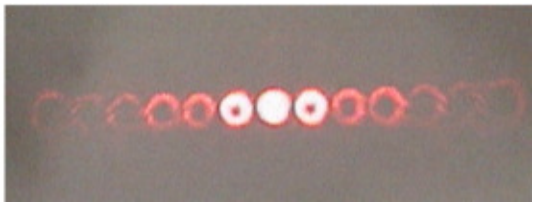

Figure 2.6: Picture of a diffraction pattern that shows the LG modes starting from $\ell = 0$ in the middle and increasing ℓ by one on each direction. Modes at opposite sides have the same ℓ but with different sign.

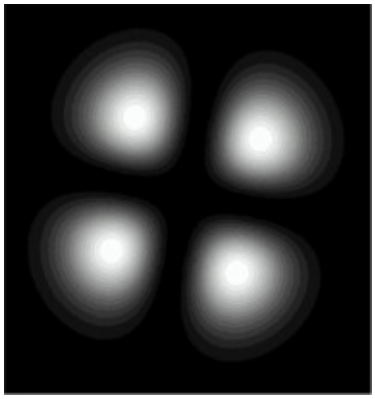

Figure 2.7: Simulation of the interference pattern between a LG_0^ℓ bean and a plane wave.

Problem 7 c. If a Gaussian beam is in an LG_0^ℓ mode, determine the value of ℓ from the interference pattern shown in Fig. 2.7. This pattern occurs at $z = 0$ when the Gaussian beam is superimposed with a plane wave of the same wavelength. The bright spots correspond to points where the two waves are in phase (also called constructive interference) and conversely the dark spots correspond to points where the waves are 180 degrees out of phase (also called destructive interference). Justify your answer.

Ans. Let us assume that the plane wave has a phase of 2π. There are four points where there is a maximum of interference, or places where the phase is a multiple of 2π, Therefore it is $\ell = 4$.

Problem 8 A Gaussian beam from a HeNe laser is incident on a lens with a focal length of 10 cm. At the lens, before being refracted, the radius of curvature of the wave is infinite and its half width is $w = 2$ mm. The total power of the beam is 5 mW.

1. What is the maximum intensity of the beam (in W/m^2) at the focal point of the wave?

   Ans. Using Eq. 1.33, $w_{02} = 1 \cdot 10^{-5}$ m, and so using Eq. 2.36, $I_{\max} = 3.18 \cdot 10^2$ W/m^2.

2. How much power will get transmitted through a 0.2-mm diameter aperture placed a distance of 1 cm from the smallest waist of the beam (focal point)?

   Ans. $z_R = 5 \cdot 10^-9$ m, $w(1\text{cm}) = 2 \cdot 10^{-4}$ m $= a_0$, (Eq. **??**), then using Eq. 1.26, we get $P = 4.3$ mW.

Problem 9 A Gaussian beam of wavelength 600 nm travels along the z-axis. It has a waist $w_0 = 0.5$ mm located at $z = 0$.

1. At what value of z will the radius of curvature of the phase front be $R = 2z$?

2. What is the intensity at point $z = z_R$, $r = 2w(z)$ relative to the intensity at $z = 0$, $r = 0$ (r is the distance from the axis of the beam).

3. Calculate the Gouy phase at $z = z_R$.

4. Calculate the phase difference between the point $(z = z_R, r = 0)$ and $(z = z_R, r = 2w(z))$.

5. If the power of the beam is 5 mW, What is the maximum intensity at $z = 5z_R$?

Problem 10 Consider the mode HG_{22} in Cartesian coordinates and the mode LG_0^4 in cylindrical coordinates.

1. Make a two-dimensional contour graph of the intensity of each mode as if it were projected on a screen. You could either use the software of choice or make the contour graph by hand like a topological map, indicating the regions of high intensity.

2. For each mode mark the regions on your graphs that have a phase that is a multiple of 2π.

Chapter 3

Wave-front interference

In this chapter we will discuss the formalism for understanding the wavefont of complex light. In the laboratory we study complex wavefronts via interference with known wavefronts. We can best do this with an amplitude dividing interferometer, such as a Mach-Zehnder interferometer in combination with wave-front reshaping optical elements in the arms of the interferometer.

3.1 General Formalism

Consider the wave-function of a beam of light to be given by the complex-notation expression

$$\Psi = Ae^{i\phi}, \tag{3.1}$$

where A is the amplitude and ϕ is the phase. The amplitude can be constant, as it is for the case of a plane wave. It can also depend on the transverse coordinates (x and y, when the wave propagates along the z-axis). For the case of a Gaussian beam the amplitude decreases with a characteristic Gaussian shape given by $\exp[-(x^2 + y^2)/w^2]$, where w is the width of the beam or beam spot. The phase of the wave can take the simple form $(kz - \omega t)$, where $k = 2\pi/\lambda$ is the wave number and ω is the angular frequency. This is the case for a plane wave traveling along the z-direction. The expression for the phase can be more elaborate and can have other terms. For example, an spherical wavefront expanding wave is accounted by the term $k(x^2+y^2)/(2R)$, where R is the radius of curvature of the wavefront. There is another phase that Gaussian beams acquire due to propagation of the light. This phase is called the Gouy phase. It is given by $\varphi = (N + 1)\tan^{-1}(z/z_R)$, where z_R is the Raleigh range and N is the order of the mode of the beam.

Let us consider two light waves Ψ_1 and Ψ_2. The interference pattern produced by

the superposition of the two waves will have an intensity given by

$$\begin{aligned} I &= |\Psi_1 + \Psi_2|^2 && (3.2)\\ &= |A_1 e^{i\phi_1} + A_2 e^{i\phi_2}|^2 && (3.3)\\ &= (A_1 e^{i\phi_1} + A_2 e^{i\phi_2})^*(A_1 e^{i\phi_1} + A_2 e^{i\phi_2}) && (3.4)\\ &= (A_1 e^{-i\phi_1} + A_2 e^{-i\phi_2})(A_1 e^{i\phi_1} + A_2 e^{i\phi_2}) && (3.5)\\ &= A_1^2 + A_2^2 + A_1 A_2 (e^{i(\phi_1-\phi_2)} + e^{-i(\phi_1-\phi_2)}) && (3.6)\\ &= A_1^2 + A_2^2 + 2A_1 A_2 \cos(\phi_1 - \phi_2). && (3.7) \end{aligned}$$

For simplicity let's consider $A_1 = A_2 = A$. In this case the intensity reduces to

$$I = 2A^2(1 + \cos\Delta\phi), \tag{3.8}$$

where

$$\Delta\phi = \phi_1 - \phi_2. \tag{3.9}$$

Constructive interference fringes satisfy

$$\Delta\phi = 2\pi n, \tag{3.10}$$

where n is an integer.

3.2 Interference of Zero-order Beams

3.2.1 Collinear Interference

A Mach-Zehnder interferometer is shown in Fig. 3.1. When the interferometer has

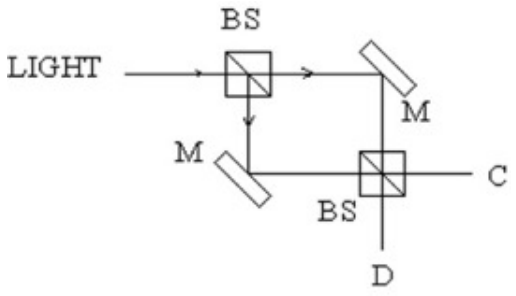

Figure 3.1: Mach-Zehnder interferometer.

50-50 beam splitters the first one divides the light into equal amplitudes traveling along the two arms. The second beam splitter recombines the light. The reflection and transmission coefficients of the beam splitters are $r = i/\sqrt{2}$ and $t = 1/\sqrt{2}$, respectively.

Exercise 6 If the wave of Eq. 3.1 is incident on a Mach-Zehnder interferometer, show that the amplitudes at the two output ports of the interferometer are:

$$\Psi_C = \frac{i}{2}(e^{i\phi_1} + e^{i\phi_2}) \tag{3.11}$$

and

$$\Psi_D = \frac{1}{2}(e^{i\phi_1} - e^{i\phi_2}). \tag{3.12}$$

Exercise 7 Show that the intensity at the ports C and D are:

$$I_C = \frac{A^2}{2}(1 + \cos\Delta\phi), \tag{3.13}$$

and

$$I_D = \frac{A^2}{2}(1 - \cos\Delta\phi). \tag{3.14}$$

Let us consider projecting the output of port C of the interferometer onto a screen or CCD camera. If the arms of the interferometer differ by a length L, then the phase difference between the light coming from the two arms of the interferometer is

$$\Delta\phi = \frac{2\pi}{\lambda}L. \tag{3.15}$$

Ignoring the two turns that the light takes in going through the interferometer we can define the phase of the light going through the two arms of the interferometer as $\phi_1 = kz_1$ and $\phi_2 = kz_2$. The beams travel distances z_1 and z_2 from the first beam splitter to the screen or CCD. The phase difference between the two beams is $\Delta\phi = \phi_1 - \phi_2 = k(z_1 - z_2) = kL$, which consistent with Eq. 3.15.

3.2.2 Noncollinear Interference

In the next case one of the beams, say beam 1, forms an angle β with the direction of propagation of beam 2, which is traveling along the z-axis. This is shown in Fig. 3.2. When a beam is incident on a screen at an oblique angle, its phase will not be constant along the plane of the screen. In the case of the beam 1 in Fig. 3.2 the phase will vary along the x-direction. The greater the value of β the greater the phase variation with x.

One can see this more formally by considering beam 1 to be a plane wave with wave-vector $\mathbf{k} = k(\sin\beta, 0, \cos\beta)$. The phase of the wave will be

$$\phi_1 = \mathbf{k}\cdot\mathbf{r} - \omega t \tag{3.16}$$

$$= kx\sin\beta + kz\cos\beta - \omega t. \tag{3.17}$$

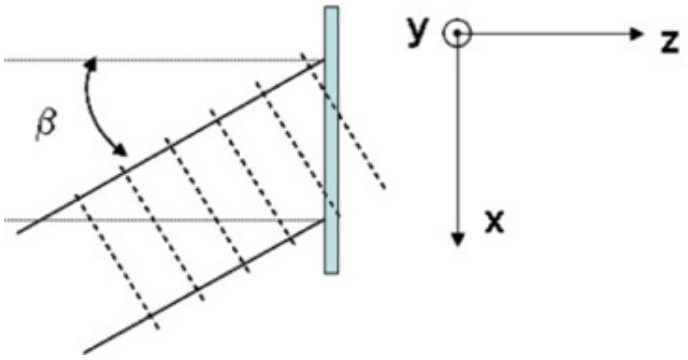

Figure 3.2: Noncollinear case of interference. Two beams with propagation directions that form an angle β meet at a screen. Dashed lines correspond constant-phase wave-fronts.

The phase difference between the two beams is

$$\Delta\phi = \frac{2\pi x}{\lambda}\sin\beta + \frac{2\pi}{\lambda}z\cos\beta - \frac{2\pi}{\lambda}(z+L). \tag{3.18}$$

The last two terms are constant at the screen. They would vary if we change the difference in length between the two arms L or the position of the screen. We can rewrite the phase difference as

$$\Delta\phi = \frac{2\pi x}{\lambda}\sin\beta + \phi(z,L), \tag{3.19}$$

where $\phi(z,L)$ contains the last two terms of Eq. 3.18. At maxima the phase difference is

$$\Delta\phi = 2\pi n. \tag{3.20}$$

The locus of points where there is constructive interference is given by

$$x = \frac{\lambda}{\sin\beta}n - x_0, \tag{3.21}$$

where $x_0 = \phi(L)\lambda/(2\pi\sin\beta)$. The fringes constitute a set of vertical lines, as sketched in Fig. 3.4 for $x_0 = 0$. The fringes are separated by a distance $\lambda/\sin\beta$. As β is

Figure 3.3: Predicted fringes when one beam forms an angle β with the other one.

increased the fringe density increases. If the path length difference L is changed then the fringes shift.

We produce these fringes by misaligning the two beams, as shown in Fig. 3.4. In actuality, it is harder to align the two beams to be collinear, so the noncollinear case is the first situation that one encounters when putting together an interferometer.

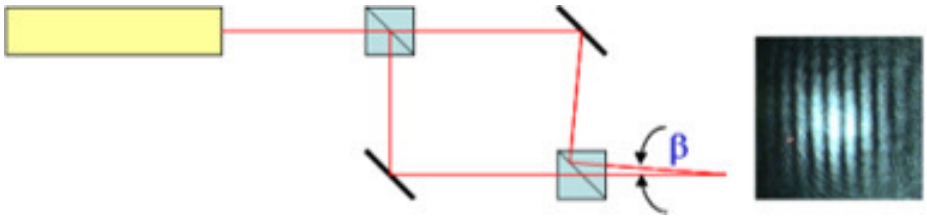

Figure 3.4: Apparatus for observing vertical fringes shown next to a sample interference pattern.

3.2.3 Interference with an Expanding Wave-front

Suppose that beam 1 is traveling along the z-axis, but is expanding. The phase of beam 1 on an XY plane will not be constant. Because the expansion of the beam implies a spherical wavefront, the phase will vary with the distance to the axis of the beam:

$$\phi_1 = \frac{k(x^2 + y^2)}{2R}, \tag{3.22}$$

where R is the radius of curvature of the wavefront. Constructive interference fringes will satisfy the relation

$$2\pi n = \frac{k(x^2 + y^2)}{2R} + \frac{2\pi}{\lambda} L. \tag{3.23}$$

This can be modified to look like the equation of a circle

$$x^2 + y^2 = r^2. \tag{3.24}$$

of radius

$$r = \sqrt{2R\lambda n - 2RL}. \tag{3.25}$$

Thus the interference pattern consists of a set of concentric circles forming a "bull's eye" pattern, as shown in Fig. 3.5. When $L = 0$ the radii of the circles increases as $\sqrt{n}$. As L is changed the circles move inwards or outwards.

We create this situation in the laboratory by putting a diverging lens in one of the arms of the interferometer, as shown in Fig. 3.6. The expanding beam will interfere with the nonexpanding beam when the two beams meet at the screen.

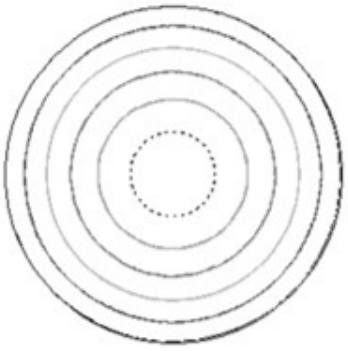

Figure 3.5: Diagram of the expected locations of circular fringes between two beams with different radii of curvature.

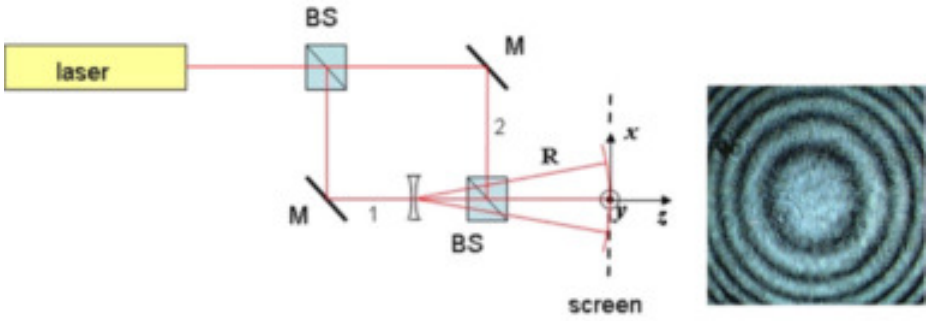

Figure 3.6: Apparatus for observing circular fringes shown next to a sample of the bull's-eye pattern.

3.3 Interference with High-Order Beams

3.3.1 Collinear Case

Now let's suppose that one of the beams is in a Laguerre-Gauss mode that has a helical wave-front. The phase of the wave then has a term of the form

$$\phi_1 = \ell\theta. \tag{3.26}$$

In this chapter we will limit ourselves to single-ringed Laguerre-Gauss beams. These have the shape of a doughnut. This is because at the center of the beam the waves with different phases interfere destructively.

We can create an interference pattern for a Laguerre-Gauss beam by using a "forked" diffraction grating in one of the arms of the interferometer. As we will see later, the forked diffraction grating is a computer-generated hologram of the interference pattern of a Laguerre-Gauss beam with a zero-order beam.

Let us first assume that the Laguerre-Gauss beam is collinear with the zero-order beam. The phase difference between the two beams is then

$$\Delta\phi = \ell\theta - \frac{2\pi}{\lambda}L. \tag{3.27}$$

Constructive interference fringes will appear at

$$\theta = \frac{2\pi}{\ell}n - \theta_0, \tag{3.28}$$

where $\theta_0 = 2\pi L/(\lambda\ell)$. When $\ell = 1$ this is just a line at a particular value of θ. For the case of a Gaussian beam, it will be a broad maximum–a "blob" at one side of the axis of the beam. This is shown in the simulation of Fig. 3.7. The value of θ_0

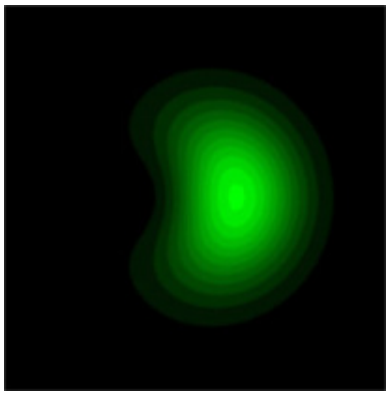

Figure 3.7: Simulation of the interference of a first-order Laguerre-Gauss beam with a zero-order beam.

increases with L. That is, the interference pattern will rotate if the path difference L changes. This is shown in the set of images of Fig. 3.8, taken in the laboratory, where the phase between the two beams was varied from one frame to the next one. Note

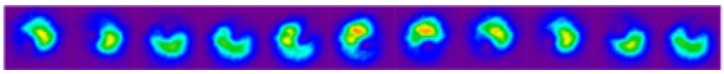

Figure 3.8: False color images of the interference of a first-order Laguerre-Gauss beam with a zero-order beam. The phase between the two beams was varied incrementally from frame to frame.

that if $\ell = -1$ then the interference will rotate in the other direction as L is changed.

Exercise 8 Sketch the interference pattern between a zero-order beam with (a) $\ell = +2$ Laguerre-Gauss beam, and (b) $\ell = -3$ Laguerre-Gauss beam.

Exercise 9 Sketch the interference pattern of a Laguerre-Gauss beam with $\ell = 1$ an an expanding beam (i.e., with a spherical wavefront.

3.3.2 Non-collinear Case

To understand the interference pattern for this case, let us first analyze the interference pattern produced by a Hermite-Gauss beam HG_{01} and a zero-order beam. The HG_{01} has two horizontal lobes. Within each lobe the phase is constant, but the two lobes are 180-degrees out of phase with respect to each other. The interference pattern between a HG_{01} beam and a zero-order beam incident at an angle consists of a set of vertical fringes. However, as shown in Fig. 3.9, the fringes of the two lobes are stagered. This stagger reflects the phase difference between the two lobes.

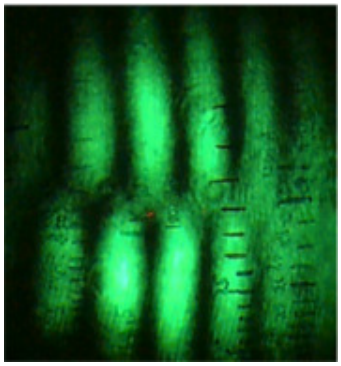

Figure 3.9: Image of the interference of a HG_{01} mode with a non-collinear zero-order mode.

Now let us consider a single-ringed $\ell = 1$ Laguerre-Gauss beam. The phase of the mode advances around the ring of the doughnut so that once we go one full turn around the center of the beam, the phase will have advanced by 2π. As a consequence, points at opposite sides from the axis of the beam are 180 degrees out of phase (e.g., directly above the center $\phi = \pi/2$, and directly below $\phi = 3\pi/2$). So points at opposite ends of the doughnut in the vertical direction should show fringes that are staggered, as seen for the case of HG_{01} mode. However, since the phase varies smoothly around the doughnut the fringes should become unstaggered as we move laterally away from the center, and connect smoothly along the sides of the doughnut (i.e., at $\theta \sim 0$ and π). Figure 3.10 shows the interference pattern of a $\ell = 1$

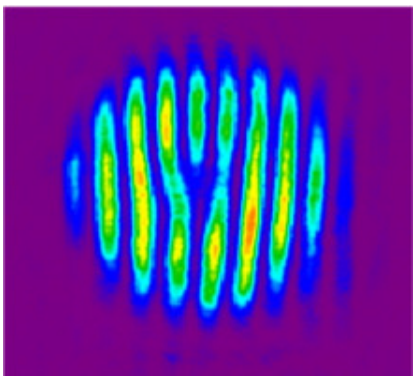

Figure 3.10: Image of the interference of a LG_0^1 mode with a non-collinear zero-order mode.

mode with a non-collinear zero-order mode. It shows a peculiar forked interference pattern. The fork is a consequence of the phase dislocation. That is, as we go around the center in a loop we gain or lose a fringe, or a phase of 2π.

Exercise 10 Using the previous argument predict the fork generated by the interference of a Laguerre-Gauss beam with $\ell = 3$ with a non-collinear zero-order beam.

Let us now proceed with a more quantitative approach. The phase difference between a Laguerre beam with "charge" (or vorticity) ℓ and a non-collinear zero-order beam is

$$\Delta\phi = \frac{2\pi}{\lambda} x \sin\beta + \ell\theta + \phi(L) \tag{3.29}$$

$$= \frac{2\pi}{\lambda} x \sin\beta + \ell \tan^{-1}\left(\frac{y}{x}\right) + \phi(L). \tag{3.30}$$

As discussed before, $\phi(L) = \frac{2\pi}{\lambda}(z\sin\beta - z + L)$ is a constant at the screen that depends on the difference in length between the two arms of the interferometer. If we graph the points satisfying $\Delta\phi = 2\pi n$ we get the patterns of Fig. 3.11. The theoretical description indeed explains the observations: the signature of a phase vortex is a fork. Notice also that the sign of the vortex is conveyed by the orientation of the fork; vortices that differ in sign produce oppositely oriented forks. The shape of the fork depends on the value of ℓ. Figure 3.12 shows how to recognize the charge ℓ of the beam that creates the fork. Each interference fringe is a change of 2π in the phase. If we start from a given point on a fringe and go in a path around the center of the fork counting fringes as we go along, we return to the initial spot having gained or lost fringes. Since the gain or loss is the difference between the fringes above the center

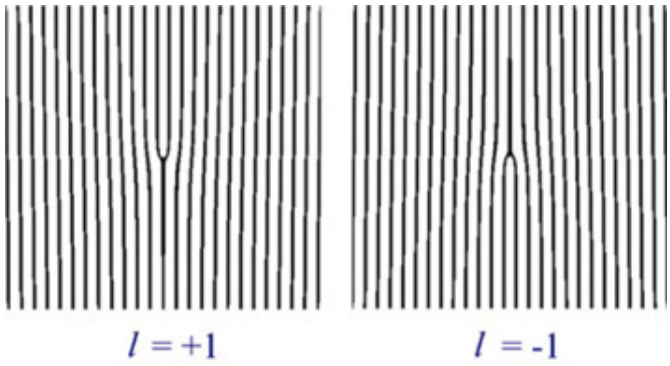

Figure 3.11: Graph of the locus of points that are in constructive interference when non collinear zero-order beam interferes with a Laguerre-Gauss beam with $\ell = +1$ (left) and $\ell = -1$ (right).

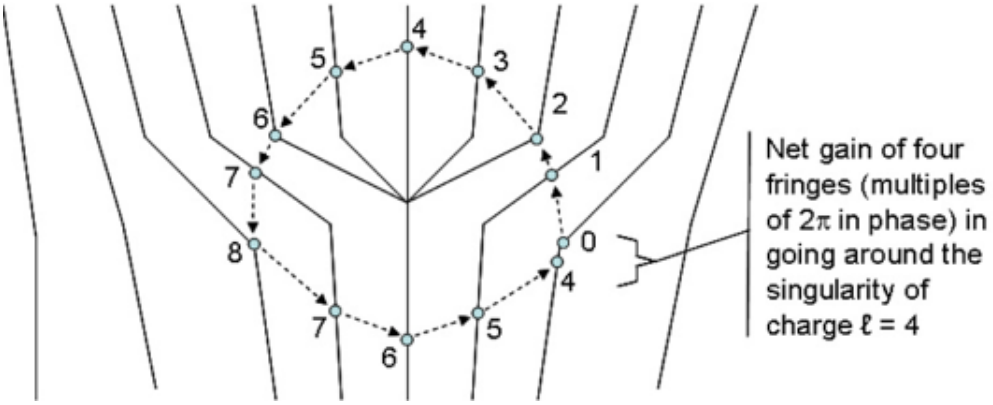

Figure 3.12: How to recognize the charge of the fork: number of tines minus one.

and those below the center, the "charge" of the fork can be recognized as the number of tines of the fork minus one. This can be verified in the computer-generated fork for $\ell = 3$, shown in Fig. 3.13

3.4 Generating Helical Beams

We conclude by discussing the generation of Laguerre-Gauss beams. There are various methods, and their use depends heavily on technology and cost.

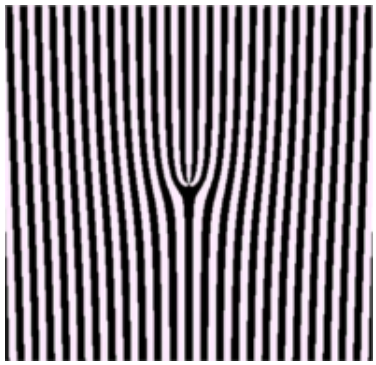

Figure 3.13: Binary hologram for generating a Laguerre-Gauss beam with $\ell = 3$ in the first diffracted order.

3.4.1 Spiral Phase Plate

The phase of the light in an ordinary laser beam is uniform and symmetric about the beam axis. The wave-fronts are either planar or spherical. One way to produce a helical beam is by brute force. That is, by introducing a phase lag as a function of the azimuthal angle. This is done with the use of a spiral phase plate, shown on the left side of Fig. 3.14.

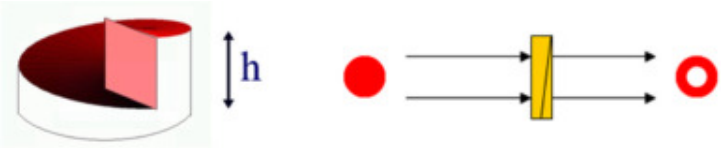

Figure 3.14: Spiral phase plate used for generating helical beams (left). It generates a helical beam by transmission through it (right).

The phase plate is made of a material with index of refraction n. It has different thicknesses at different angles. A beam of light going through it will experience phase shifts that depend on the thickness, which depends on the angle:

$$\Delta\phi = \frac{2\pi(n-1)x}{\lambda}, \tag{3.31}$$

where x is the thickness increment of the phase plate at a particular angle from the minimum thickness. In order to get a helical beam of order ℓ the largest thickness increment h (see Fig. 3.14 must produce a phase shift $\Delta\phi = 2\pi\ell$, and thus be given by

$$h = \frac{\ell\lambda}{n-1}. \tag{3.32}$$

There is one caveat: in practice the efficiency for making a given LG beam depends on the details [see M.W. Beijersbergen *et al.* Optics Communications 112, 321 (1994)]. For example, 78% of an LG_0^0 gets converted into a LG_0^1, but a higher efficiency (90's %) is obtained when converting LG_0^ℓ to $\mathrm{LG}_0^{\ell+1}$.

3.4.2 The Spatial Light Modulator

The spatial light modulator (SLM) is a pixelated electro-optic phase retarder. Without getting into too many technical details, it works the following way. It has a slab of liquid crystal molecules "sandwiched" in between two electrodes. One electrode is a transparent conducting plane. The other electrode consists of a matrix of electrically addressable conducting pads. When a voltage is applied between each of the pads and the continuous plane, the index of refraction of the liquid-crystal medium is altered. If different pads have different voltages, then light going through the medium experiences a transverse-position-dependent phase shift. As a consequence, the wavefront of the light going through the SLM is modified. If we program the SLM with a spiral phase pattern of phase, as shown in Fig. 3.15, then the reflected beam will experience a wavefron reconstruction similar to the case of a spiral phase plate.

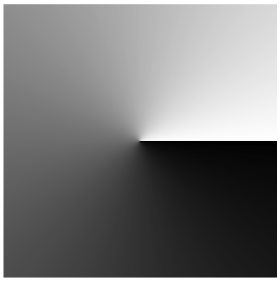

Figure 3.15: Spiral phase encoded in gray scale (white=0, black=2π) for programing the SLM to produce an $\ell = +1$ Laguerre-Gauss mode upon reflection.

If one puts a photographic film on the screen where the fringes are projected, and develop the film, the result is a diffraction grating with "slits" (that is, places where film is not exposed) separated by a distance

$$d = \lambda / \sin\beta. \tag{3.33}$$

If we shine a zero-order beam to this photographic grating we get that the first-order diffracted beam appears at an angle given by the formula for diffraction:

$$\sin\theta = \lambda / d. \tag{3.34}$$

Comparing Eqs. 3.35 and 3.36 we get that $\theta = \beta$! This is the principle of holography. The pattern recorded on the film is the hologram of the beam coming at the angle β. When shining the "reference" beam (the one normal to the pattern) onto the grating we get the holographic reconstruction coming at the angle of the original beam: β.

3.4.3 Diffraction Gratings

Holography

If one puts a photographic film on the screen where the fringes are projected, and develop the film, the result is a diffraction grating with "slits" (that is, places where film is not exposed) separated by a distance

$$d = \lambda / \sin\beta. \tag{3.35}$$

If we shine a zero-order beam to this photographic grating we get that the first-order diffracted beam appears at an angle given by the formula for diffraction:

$$\sin\theta = \lambda / d. \tag{3.36}$$

Comparing Eqs. 3.35 and 3.36 we get that $\theta = \beta$! This is the principle of holography. The pattern recorded on the film is the hologram of the beam coming at the angle β. When shining the "reference" beam (the one normal to the pattern) onto the grating we get the holographic reconstruction coming at the angle of the original beam: β.

Amplitude Gratings

As we have discussed previously, a developed interference pattern serves as a hologram. Since we know the mathematical form of the interference pattern we can calculate it, photo-reduce it, and use it as a grating. A binary grating for generating $\ell = 3$ is shown in Fig. 3.13.

The holographic reconstruction consists of simply sending a zero-order beam through a forked grating. As shown in Fig. 3.16 for a fork of charge 1, the reconstructed beams come in the first order diffraction. However, the binary grating produces much more: in the higher diffracted orders we also get higher-order beams. That is, in the n-th diffracted order we get we get a beam with a charge n. At opposite sides of the zero order the beams have the opposite helicity.

We can generalize the diffraction off a forked grating in a very interesting way. The separation Δx between fringes in a forked grating satisfies

$$2\pi = \frac{2\pi}{\lambda}\Delta x \sin\beta + \ell\Delta\theta. \tag{3.37}$$

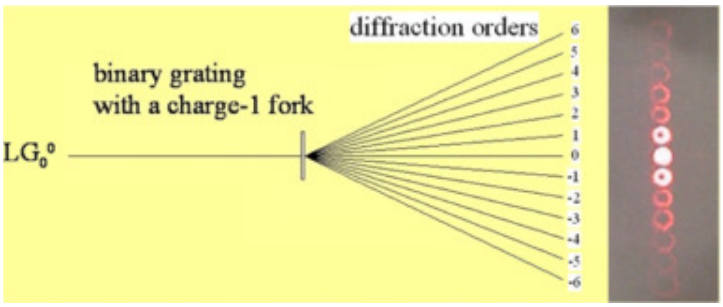

Figure 3.16: Sending a zero-order beam through a charge-1 binary forked grating.

The second term is responsible for the higher density of fringes above and below the center of the fork. The average fringe separation is given by

$$\Delta x_0 = \frac{\lambda}{\sin\beta}. \tag{3.38}$$

Rewriting Eq. 3.37 gives

$$\Delta x = \Delta x_0 - \frac{\ell \Delta\theta \Delta x_0}{2\pi}. \tag{3.39}$$

When a zero order beam is diffracted by the forked grating we get beams diffracted at angles α that satisfy

$$\sin\alpha = \frac{n\lambda}{\Delta x_0}. \tag{3.40}$$

The diffracted light appears at angles specified by the average fringe separation. When analyzing diffracted light one usually considers the phase difference due to rays from adjacent slits (Fig. 3.17). This phase difference is given by $\Delta\phi = k\Delta x \sin\alpha$. Using

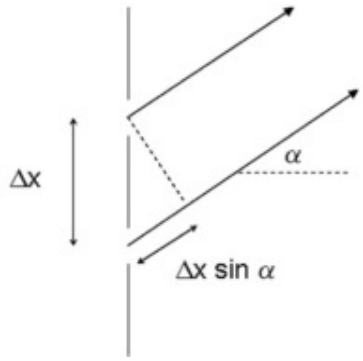

Figure 3.17: Schematic of two rays leaving adjacent slits of a diffraction grating at an angle α.

Eqs. 3.39 and 3.40 we get that the phase between adjacent rays is given by

$$\Delta\phi = 2n\pi - n\ell\Delta\theta. \tag{3.41}$$

The equation implies that the helicity of the diffracted beam is given by $n\ell$. More interestingly, if the beam incident on the grating has a helicity ℓ' then Eq. 3.41 becomes

$$\Delta\phi = 2n\pi - (\ell' + n\ell)\Delta\theta. \tag{3.42}$$

Equation 3.42 implies that in the general case of an incoming beam of helicity ℓ_{inc} incident on a forked grating of charge ℓ_{fork}, the diffracted beam has a helicity

$$\ell_{\text{diff}} = \ell_{\text{inc}} + n\ell_{\text{fork}}. \tag{3.43}$$

One could view this relation in a different way: as conservation of angular momentum. The fork imparts an angular momentum given by $n\ell_{\text{fork}}$. Thus the total angular momentum of the beam is the incident momentum plus the one given by the fork. It is interesting that one could use this to determine the helicity of the incoming light: the diffracted order that yields $\ell_{\text{diff}} = 0$ indicates that $\ell_{\text{inc}} = \ell_{\text{fork}}/n$. This relation has been demonstrated recently, as shown in Fig. 3.18.

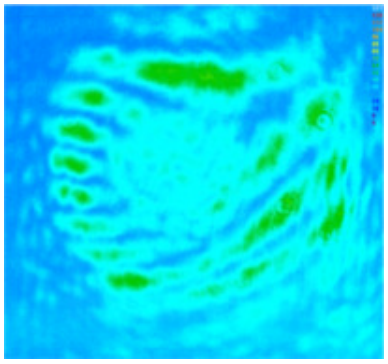

Figure 3.18: Diffraction pattern produced by $\ell_{inc} = 1$, $\ell_{fork} = 2$ and $n = 2$. The pattern contains a fork with $\ell_{diff} = 4$, in agreement with Eq. 3.43 (Galvez and Baumann, in Proc. SPIE, 2007).

To diagnose the phase of a helical beam we place the fork in one of the arms of the interferometer and steer the beams such that the first diffracted order going through one arm is sent in a direction that is collinear with the zero-order coming from the other arm. Alternatively, we can place the grating before the interferometer and have the Mach-Zehnder components steer the first and zero orders so that they overlap at the screen. This is shown in Fig. 3.19

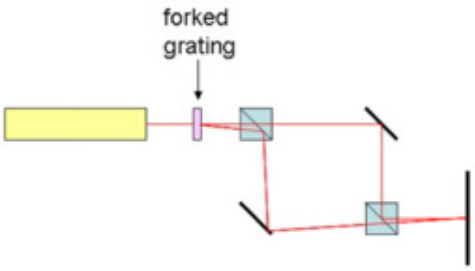

Figure 3.19: Setup to investigate the phase properties of Laguerre-Gauss beams.

One of the weaknesses of the binary diffraction grating is that since it spreads out the light into a large number of orders. If we wish to obtain one particular beam the efficiency is low, and is determined by the slit function of the grating. For example if the ratio of dark to light fringe thickness is 1, then the even diffraction orders are suppressed. A more efficient way to produce beams in definite LG modes is by use of phase gratings.

Phase Gratings

This topic is most rigorously treated by a Fourier treatment of the problem. Short of that we will try to explain phase interference using the same arguments as before. This type of interference has become important with the widespread use of spatial light modulators (SLM). Suppose that a holographic film imparts a phase onto the beam $\phi'(x, y)$. The light beam (a plane wave, for simplicity) will emerge from the optical element with a phase

$$\phi = kz + \phi'. \tag{3.44}$$

Following the previous discussion, suppose that the phase imparted on the light is a simple continuous phase:

$$\phi' = \frac{2\pi}{\lambda} \sin \beta x = k \sin \beta x. \tag{3.45}$$

The emerging beam has a phase

$$\phi = \mathbf{k}' \cdot \mathbf{r}, \tag{3.46}$$

where $\mathbf{k}' = (\sin \beta, 0, 1)$. For small angles we can say that $1 \sim \cos \beta$, so that the "new" wavevector after the film, $\mathbf{k}'$, is in a direction that forms an angle β with the original direction. That is, it acts as a beam deflector. Most phase-SLMs are reflective, so the beam coming out of the SLM is reflected but an angle β, and the SLM acts like

a mirror. The distinction between this and a diffraction grating is very small. Small imperfections in the pattern make it a grating, but a blazed grating, That is a grating where most of the intensity goes on to the diffracted order where the SLM acts as a phase reflector.

Now consider a different situation: a binary phase grating: we program a set of N (odd) stripes separated by a distance d where adjacent stripes have relative phase ϕ. This is represented in Fig. 3.20(a). The light diffracted at an angle θ (Fig. 3.20(b)

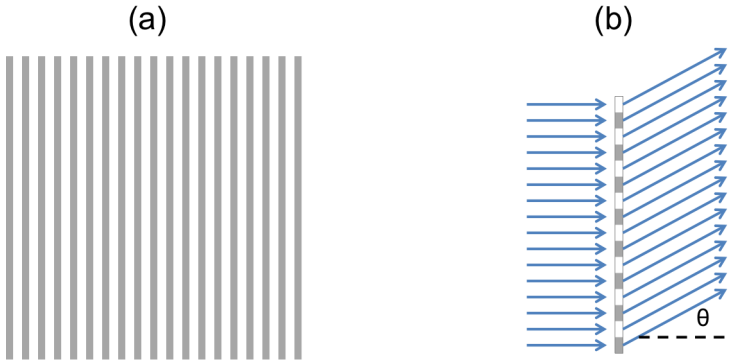

Figure 3.20: A phase diffraction grating (a) where light going through areas with distinct shade acquire a distinct phase. The diffracted beam (b) will be affected by the phase of the stripes.

can be modeled as a sum of waves coming from each section of the grating.

$$E = E_0 + E_0 e^{i(\delta+\phi)} + E_0 e^{i(2\delta+\phi)} + E_0 e^{i(3\delta+\phi)} + \cdots \tag{3.47}$$

where $\delta = kd\sin\theta$. Factorizing, the field becomes

$$E = E_0 \sum_{n=0}^{N/2} e^{i2n\delta}(1 + e^{i(\delta+\phi)}), \tag{3.48}$$

which after some algebra yields

$$E = 2E_0 e^{i\alpha} \frac{\sin[(N+1)\delta/2]}{\sin\delta} \cos[(\delta+\phi)/2], \tag{3.49}$$

where $\alpha = N\delta/2 + \phi/2$. The first diffracted order appears when $\delta = \pi$. The intensity of this order is given by

$$I = I_0(1 - \cos\phi)/2 \tag{3.50}$$

This fact is used to calibrate the phase of the SLM.

3.5 Superposition of Optical Beams

Something to note is that the beams that are produced by interference and projected onto a screen are optical beams in themselves, and can have interesting phase patterns. For example, the pattern of Fig. 3.7, which is the interference of two beams, one with a phase vortex and the other with a constant phase, results in a mode that has an off axis phase, as shown in Fig. 3.21(a). If both beams have a vortex, of charge ℓ_1 and ℓ_2 (with $|\ell_1| < |\ell_2|$), then the resulting beam is quite interesting: it has a vortex of charge ℓ_1 in the center with $|\ell_2 - \ell_1|$ singly charged vortices (of same sign as ℓ_2) evenly distributed around the center of the beam. An example of the phase for the superposition of two beams is shown in Fig. 3.21(b).

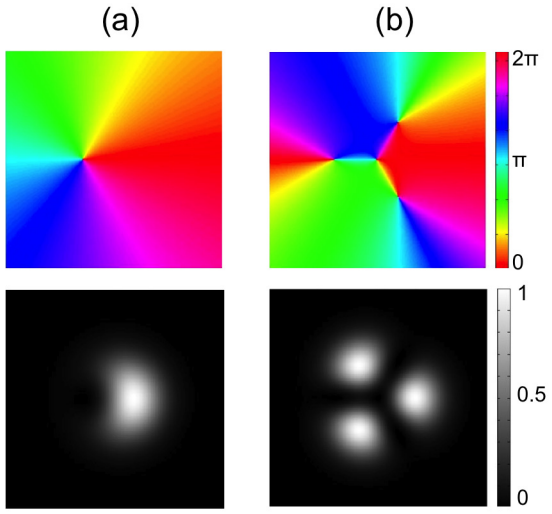

Figure 3.21: Two cases of superposition of beams carrying an optical vortex: (a) $\ell_1 = 0$ and $\ell_2 = +1$; and (b) $\ell_1 = 2$ and $\ell_2 = -1$. The top two images show the color-coded phase of the beams. The bottom two images show the absolute value of the amplitude of the beam.

This can be understood simply by analyzing the component spatial modes. If we have two vortex beams of different order, they have different radial profiles and so there is a radius r_v where they have the same amplitude. Since the beams have phases that evolve at different rates, there will be $|\ell_1 - \ell_2$ angles at radius r_v where the phase difference between the two beams will be π, and so there will be destructive interference. Those points will have a vortex. They are shown in Fig. 3.21(b) for the case where $\ell_1 = 2$ and $\ell_2 = -1$.

At the center of the composite beam the mode that has the lower value of *ell* will have a greater amplitude for $r > 0$, so the vortex at the center will have the charge of

that of the smaller of the two values of ℓ (in absolute value). Note also that the rate at which the phase advances is different for the central and "peripheral" vortices.

Moreover, if we change the overall relative phase between the two modes, the entire pattern rotates. Since modes of distinct order accumulate different Gouy phases upon propagation, the pattern will also rotate as the light propagates. If the relative power of the two beams is varied, r_v increases or decreases.

Finally, if the two modes are of the same order but with opposite charge, then there are no vortices if they have the same amplitude. They have a single central vortex, of the mode with the greatest power at the center otherwise.

3.6 Problems

Problem 11 Explain the experimental arrangement that gave rise to the following pattern. specify the possible angular momentum of the interfering beams.

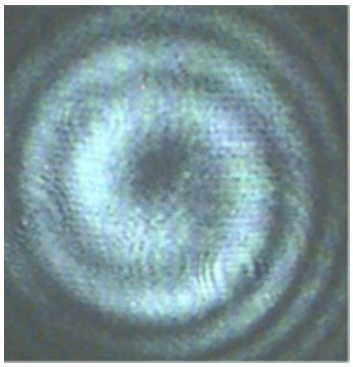

Figure 3.22: Interference pattern recorded by a CCD camera.

Problem 12 An interference pattern is made using two plane waves. They are projected on a screen as shown in Fig. 3.23.

1. Make a rigorous derivation of the fringe spacing on the screen as a function of the angle θ and the wavelength λ.

2. Figure 3.24 corresponds to an interference pattern made by Jessica Frank 01 as part of her capstone project. If the wavelength was $\lambda = 457.8$ nm, what angle θ did she used?

3. Make a detailed sketch of an optical layout she might have used in the laboratory to make this pattern. The source of light is a laser beam.

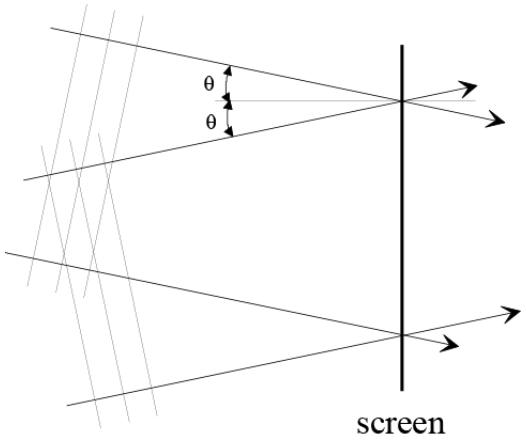

Figure 3.23: Interference pattern recorded by a CCD camera.

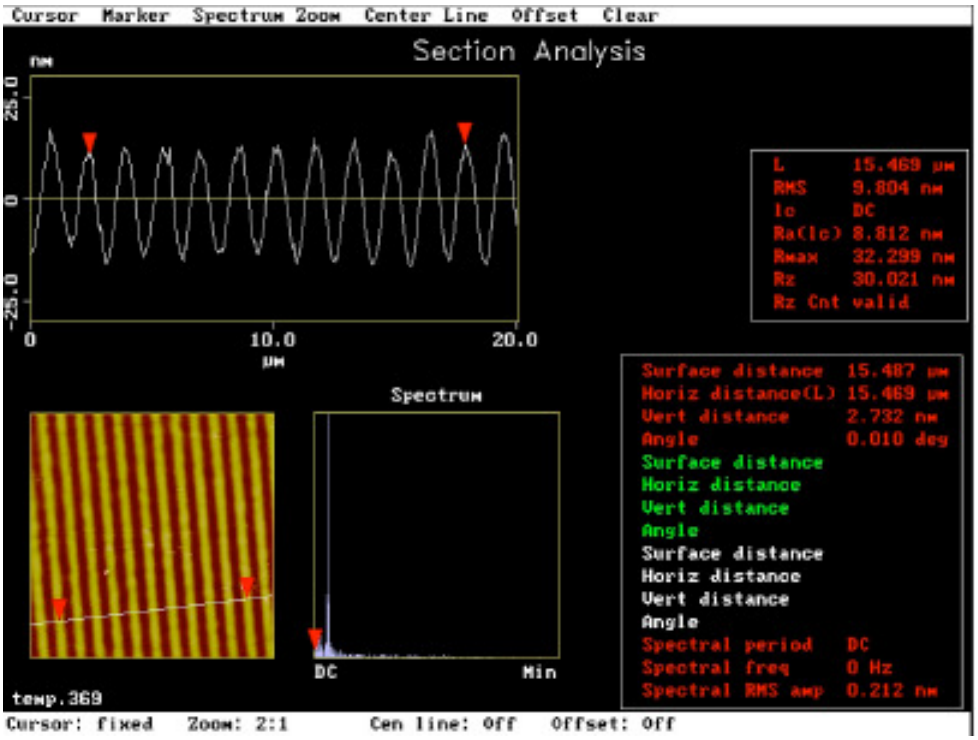

Figure 3.24: Interference pattern recorded by a CCD camera.

Chapter 4

Polarization Modes

4.1 States of Polarization

The electric field of a propagating electromagnetic wave oscillates linearly in plane that is transverse to the propagation. The most common state of polarization is linear, where the electric field oscillates in a single plane that contains the propagation direction, as shown in Fig. 4.1(a). If we denote the state of linear polarization along the x-direction by $\hat{e}_x$, and similarly, for the linear polarization along y-direction by $\hat{e}_y$, then an electric field oscillating along a direction forming an angle ϕ with the x-direction can be described by

$$E = E_0 \hat{e}_\phi \tag{4.1}$$

where

$$\hat{e}_\phi = \hat{e}_x \cos\phi + \hat{e}_y \sin\phi. \tag{4.2}$$

This polarization state is normalized if $\hat{e}_x$ and $\hat{e}_y$ are normalized. We can also denote by $\hat{e}_{x'}$ and $\hat{e}_{y'}$ respectively to the x and y polarizations rotated by an angle θ, as defined by

$$\hat{e}_{x'} = \hat{e}_x \cos\theta + \hat{e}_y \sin\theta \tag{4.3}$$

and

$$\hat{e}_{y'} = -\hat{e}_x \sin\theta + \hat{e}_y \cos\theta. \tag{4.4}$$

This is also shown in Fig 4.2. An important case is when $\theta = \pi/4$, where the unit vectors are also known as the "diagonal" and "anti-diagonal" states. They are given by

$$\hat{e}_D = \frac{1}{\sqrt{2}}(\hat{e}_x + \hat{e}_y) \tag{4.5}$$

and

$$\hat{e}_A = \frac{1}{\sqrt{2}}(-\hat{e}_x + \hat{e}_y). \tag{4.6}$$

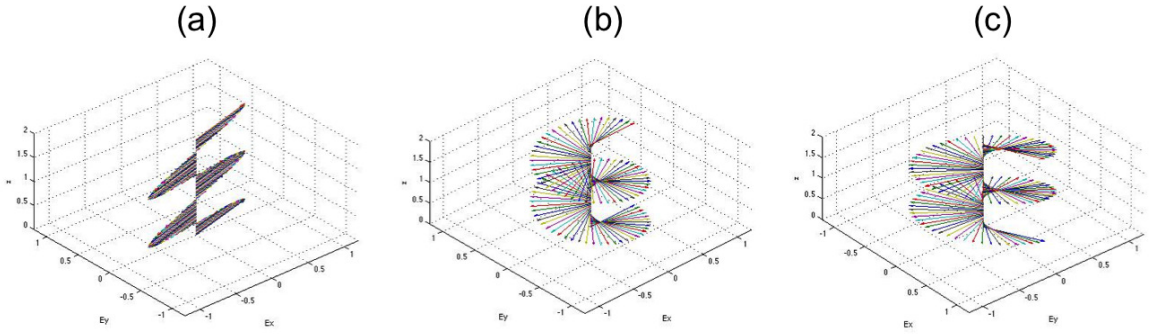

Figure 4.1: Plots of the electric field as a function of the propagation direction for a given fixed time. It shows three distinct states of polarization: (a) linear, (b) circular, and (c) elliptical.

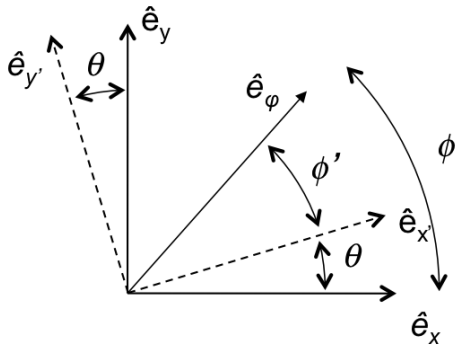

Figure 4.2: Linear polarization state representation from two reference frames rotated by θ about the origin.

If $\theta = \pi/2$ and the states (waves) are out of phase by $\pi/2$, the electric field no longer oscillates, but rotates, with the tip of the vector describing a circle, as shown in Fig. 4.1(b). This is known as circular polarization. Depending on whether the phase is positive or negative, the electric field rotates in one sense or the other, and so we call right and left circular polarization when the electric field rotates clockwise and counter clockwise, respectively, as a function of time in a given transverse plane when we are looking into the beam of light. The states of right (R) and left (L) circular polarization can be described in terms of the linear states as:

$$\hat{e}_R = \frac{1}{\sqrt{2}}(\hat{e}_x - i\hat{e}_y) \tag{4.7}$$

and

$$\hat{e}_L = \frac{1}{\sqrt{2}}(\hat{e}_x + i\hat{e}_y), \tag{4.8}$$

respectively. The complex factor is $i = exp(i\pi/2)$, which represents a phase of $\pi/2$ between the two components.

If the maximum amplitudes of the x and y components are not the same, or if the phase between them is not a multiple of $\pi/2$, then the electric field describes an ellipse, as shown in Fig. 4.1(c). In the most general case, both occurrences are true. A general elliptically polarized state is an ellipse with its semi-major and semi-minor axes rotated. A convenient way to represent an elliptical state is in terms of the two circular states:

$$\hat{e}_{\theta,\chi} = \hat{e}_R e^{+i\theta}\cos\chi + \hat{e}_L e^{-i\theta}\sin\chi. \tag{4.9}$$

It is convenient because the ratio of the amplitudes, expressed by the angle χ controls the degree of ellipticity, and the phase in between them controls the orientation of the axes. The Poincaré sphere of Fig. 4.3 is a convenient means geometrical construction that allows us to represent all the states of polarization by points on the surface of the sphere. Angle χ is half of the polar angle, and so the latitude on the sphere is given by $\pi/2 - 2\chi$. Angle θ is half the azimuthal angle, or longitude on the sphere, as shown in Fig. 4.3. The north and south poles are the states of right and left circular

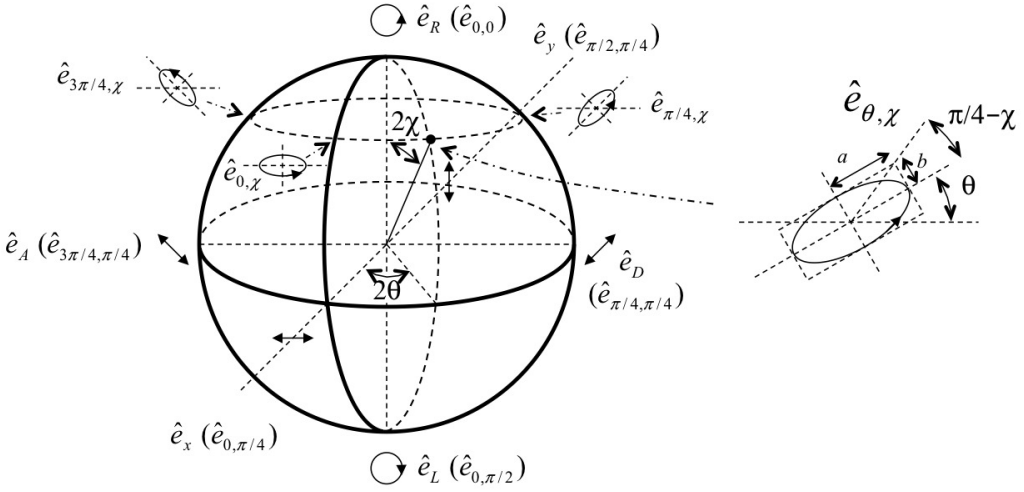

Figure 4.3: The Poincaré sphere. All the states of polarization are represented by points on the surface.

polarization, respectively. All the points along the equatorial line are states of linear polarization with orientations that depend on the azimuth angle. Points in between,

in the northern and southern hemispheres are states of elliptical polarization with right and left handedness, respectively. The full array of states is shown in Fig. 4.4.

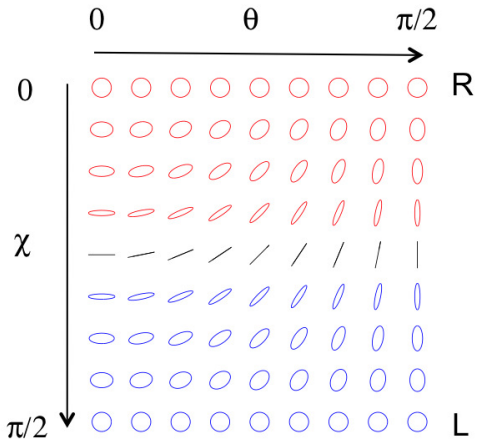

Figure 4.4: All the states of polarization are represented by the polar angles on the Poincaré sphere.

When the elliptically polarized state has its axes aligned with the Cartesian axes x and y, the state is be represented by $\hat{e}_{0,\chi}$ in Fig 4.3. This state is given by

$$\hat{e}_{0,\chi} = \cos\chi\ \hat{e}_R + \sin\chi\ \hat{e}_L. \tag{4.10}$$

By replacing Eqs. 4.7 and 4.8 into Eq. 4.10 we can express the state in terms of the linear states along x and y:

$$\hat{e}_{0,\chi} = \cos(\pi/4 - \chi)\ \hat{e}_x - i\sin(\pi/4 - \chi)\ \hat{e}_y. \tag{4.11}$$

This is the equation of an ellipse with an ellipticity

$$\epsilon = \tan(\pi/4 - \chi) = \frac{b}{a}, \tag{4.12}$$

where b and a are the semi-minor and semi-major axes of the ellipse, respectively.

We obtain the more general case of an elliptically polarized state by rotating the axes of the ellipse by an angle θ. Analytically, we rotate the state of Eq. 4.11 by θ. Since the amplitude of components relate only to the ellipticity and not the orientation of the ellipse, we can express the rotated state as the same ellipse but relative to rotated axes:

$$\hat{e}_{\theta,\chi} = \cos(\pi/4 - \chi)\ \hat{e}_{x'} - i\sin(\pi/4 - \chi)\ \hat{e}_{y'}, \tag{4.13}$$

where $\hat{e}_{x'}$ and $\hat{e}_{y'}$ are given by Eqs. 4.3 and 4.4, respectively. This state is represented on the Poincaré sphere by the point with azimuth angle 2θ and polar angle 2χ, as shown in Fig 4.3. By expressing $\hat{e}_{x'}$ and $\hat{e}_{y'}$ in terms of $\hat{e}_R$ and $\hat{e}_L$ it can be shown that Eq. 4.13 reduces to Eq. 4.9.

The notation of Eq. 4.9 then calls for the following associations: $\hat{e}_x = \hat{e}_{0,\pi/4}$, $\hat{e}_y = \hat{e}_{\pi/2,\pi/4}$, $\hat{e}_D = \hat{e}_{\pi/4,\pi/4}$, $\hat{e}_A = \hat{e}_{3\pi/4,\pi/4}$, $\hat{e}_R = \hat{e}_{0,0}$, and $\hat{e}_L = \hat{e}_{0,\pi/2}$. A state of linear polarization rotated by θ is given by

$$\hat{e}_{\theta,\pi/4} = \frac{1}{\sqrt{2}}(\hat{e}_R e^{+i\theta} + \hat{e}_L e^{-i\theta}). \tag{4.14}$$

4.2 Mode and Polarization Combinations

This section combines the results from the previous section on states of polarization with the discussion in the Chapter 3 regarding superposition: that superposition of modes yields a new mode with a variety of amplitudes and phases. A few combinations are worthy of notice.

4.2.1 Vector Beams

Let us combing Hermite-Gauss modes in distinct states of linear polarization:

$$V = \frac{1}{\sqrt{2}}(HG_{10}\hat{e}_{x'} + e^{i\alpha}HG_{01}\hat{e}_{y'}), \tag{4.15}$$

where α is the relative phase between the two modes. The states of polarization $\hat{e}_{x'}$ and $\hat{e}_{y'}$ are linearly polarized states parallel to a set of orthogonal axes rotated by θ relative to x and y, respectively. When $\alpha = 0$ the mode can be expressed as

$$V = \frac{1}{\sqrt{2}}(HG_{10}\hat{e}_{x'} + HG_{01}\hat{e}_{y'}), \tag{4.16}$$

Replacing expressions for the Hermite-Gauss Modes, Eqs. 2.22 and 2.23:

$$V = \frac{1}{\sqrt{2}}(x\hat{e}_{x'} + y\hat{e}_{y'})B_1 GW, \tag{4.17}$$

but $x = r\cos\phi$ and $y = r\sin\phi$, so

$$V = \frac{1}{\sqrt{2}}(\cos\theta\ \hat{e}_{x'} + \sin\theta\ \hat{e}_{y'})rB_1 GW. \tag{4.18}$$

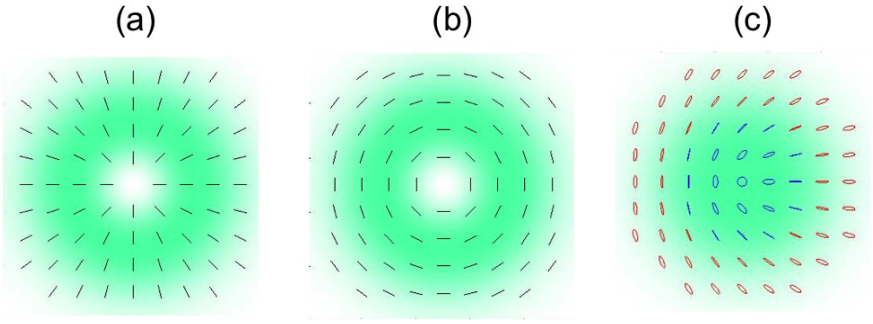

Figure 4.5: Light modes where the state of polarization varies across the beam profile: (a) radial vector beam, (b) azimuthal vector beam, and (c) Poincare beam. For the latter case, the handedness of the state is encoded in color: red is left-handed and blue is right-handed.

From Eq. 4.3 this state is the linear polarization making an angle ϕ relative to the coordinate axis x', which is rotated by θ. Therefore,

$$V = \frac{1}{\sqrt{2}} r B_1 G W \; \hat{e}_{\phi+\theta}. \tag{4.19}$$

Before we analyze this result, we note that this same state can ve obtained via:

$$V = \frac{1}{\sqrt{2}} (L G_0^{+1} e^{i\theta} \hat{e}_R + L G_0^{-1} e^{-i\theta} \hat{e}_L), \tag{4.20}$$

Let us set $\theta = 0$ for now. This is equivalent to the case $x' = x$ and $y' = y$. Note the state of polarization. Since ϕ is the angular coordinate, at a point of radius r and angle ϕ the polarization is linear and oriented in the radial direction, as shown in Fig. 4.5(a). The product rG gives an amplitude consisting of a single ring.

When $\theta = \pi/2$, the state is in a mode with a linear polarization given by $\hat{e}_{\phi+\pi/2}$ where the orientation of the polarization is always perpendicular to the radial direction, or tangential to the ring of the mode, as shown in Fig. 4.5(b). It can be expressed formally as:

$$V = A_1 r \; G \; W \; \hat{e}_{\phi+\pi/2}. \tag{4.21}$$

This type of vector beam is known as the azimuthally or tangentially polarized vector beam.

A unique aspect of the radial and azimuthal vector beams is that they contain only linearly polarized states. What varies is only the orientation. If you analyze Eq. 4.14, you will realize that it serves to understand this. This is because the superposition of the two circular states with equal amplitudes gives rise to a linear state, with the

orientation given by half the phase difference between the states. Modes LG_0^{+1} and LG_0^{-1} have amplitudes with the same radial dependence (see, for example, Eq. 2.25), and hence the superposition of Eq. 4.20 has to give linear states. Because the phase of LG_0^{+1} increases counter-clockwise and that of LG_0^{-1} increases clockwise, the relative phase between the two circular components at a given point (r, ϕ) is 2ϕ, and so the orientation of the linear state is ϕ (i.e., the radial mode). If in addition, the two modes have a relative phase 2θ then the relative phase between the two modes is $2(\phi+\theta)$, and so, when $\theta = \pi/2$ the orientation of the linear state is orthogonal to the radial direction (i.e., azimuthal polarization).

4.2.2 Poincaré Beams

Now let us cnsider another combination of modes and polarization. This time we will start with the Laguerre-Gauss and circular polarization bases, similar to Eq. 4.20. The only difference is that now the superposition is between two very different spatial modes: LG_0^{+1} and LG_0^0. The equation for the mode is

$$V = \frac{1}{\sqrt{2}}(LG_0^{+1}e^{-i\theta}\hat{e}_R + LG_0^0 e^{i\theta}\hat{e}_L), \tag{4.22}$$

The amplitude of these spatial modes do not have the same radial dependence. In fact, at $r = 0$ the amplitude of LG_0^{+1} is 0, while that of LG_0^0 is maximum. Thus, at $r = 0$ the state of polarization is left circular. As a function of r, the amplitude of LG_0^{+1} increases while the amplitude of LG_0^0 decreases. Thus, at a certain radius r_v they will be equal, and so the polarization will be linear. At $0 < r < r_v$ the polarization will be left-handed elliptical, with ellipticity that depends on r. For $r > r_v$ the amplitude of LG_0^{+1} will be greater than that of LG_0^0, and so the state of polarization will be right-handed, at at $r \to \infty$ right circular. Mode LG_0^{+1} has a phase that varies with ϕ whereas LG_0^0 has a constant phase. Therefore, the relative phase is at a point (r, ϕ) is $\phi + 2\theta$, and so the orientation of the elliptic-linear states is $\phi/2 + \theta$. In all, this new mode has an ellipticity that varies with radius and an orientation that varies with ϕ. It contains a mapping of all the states on the Poincaré sphere to the transverse beam mode, and for that they are called Poincaré beams. The case with $\theta = 0$ is shown in Fig. 4.5(c). The pattern rotates with θ, but only for this case. There are more interesting intricacies in these space-variant polarization modes, but they are beyond the scope of this discussion.

Chapter 5

Energy and Momentum

5.1 Energy

Fundamentals of electromagnetic waves propagating in vacuum yield the relation

$$E = cB, \tag{5.1}$$

where E and B are the amplitudes of the electric and magnetic fields, respectively. The speed of light c is given by

$$c = 1/\sqrt{\epsilon_0 \mu_0}, \tag{5.2}$$

where ϵ_0 and μ_0 are respectively the permitivity and permeability of vacuum. The electromagnetic energy density is given by the sum of the electric and magnetic energy densities:

$$U = U_E + U_B \tag{5.3}$$

$$U = \frac{1}{2}\epsilon_0 E^2 + \frac{1}{2\mu_0} B^2. \tag{5.4}$$

Exercise 11 Show that by using the relations 5.1 and 5.2 we get the energy density to become

$$U = c\epsilon_0 EB. \tag{5.5}$$

The total energy crossing an area A in a time Δt is

$$\Delta U = U A c \Delta t. \tag{5.6}$$

From the previous equation we get that the energy flowing per unit area per unit time is

$$S = \frac{\Delta U}{A\Delta t} = cU = \epsilon_0 c^2 EB. \tag{5.7}$$

The flow of energy can be expressed vectorially by the Poynting vector

$$\mathbf{S} = \epsilon_0 c^2 \mathbf{E} \times \mathbf{B}. \tag{5.8}$$

The energy carried by the electromagnetic field can thus be transported through space and delivered at remote locations. Our daily lives are importantly affected by the energy carried by the electromagnetic waves, from the heating of our planet by the Sun, to radio communications via cellular phones. Gaussian beams restricted to narrow solid angles can be used to effectively channel energy.

Gaussian beams produced by lasers can be used for interesting purposes. An interesting case is the one of adaptive-optics-based astronomy. In this case a laser beam is sent up to the atmosphere to a region within the field of view of a telescope. The light excites a well defined area in the sodium layer of the upper atmosphere, and the fluorescence of the excited region can be seen by the telescope. While the image should be that of a point source, the atmospheric inhomogeneities distort the wavefront of the light, causing decreased resolution and blurring of the image. A deformable mirror in the ground telescope readjusts its shape via actuators to give a sharp image of the beacon, which we know is a point source. This effectively negates the wave-front distortion caused by the atmosphere, and along the way sharpens the other objects in the field of view of the telescope. Figure 5.1a shows the Keck telescope with its laser beacon ($\lambda = 589$ nm). Figures 5.1b and 5.1c show images of Neptune with and without adaptive optics.

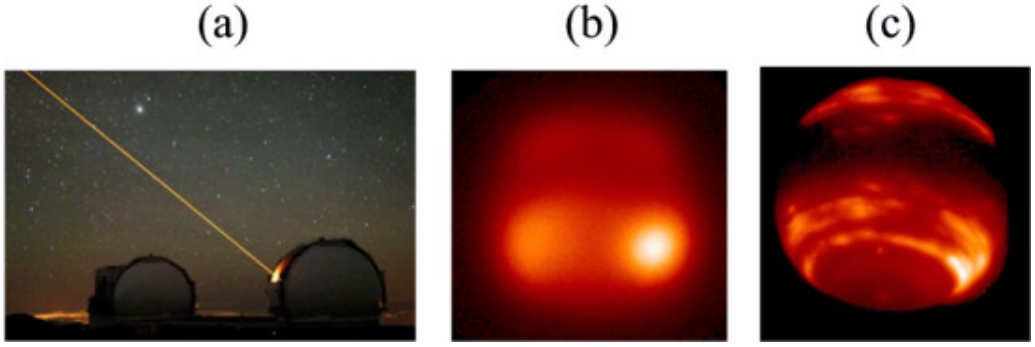

Figure 5.1: Adaptive optics technology used in the Keck telescope (a), showing the image of Neptune with (b) and without adaptive-optics-correction. Courtesy W.M. Keck Observatory.

The irradiance is the time averaged energy flow

$$I =< S >= \frac{\epsilon_0 c}{2} E_0^2, \tag{5.9}$$

where E_0 is the amplitude of the electric field. For example, the Sun produces an irradiance of 100 mW/cm^2 on the Earth's surface. A magnifying glass with an area of 25 cm^2 concentrates 2.5 W of energy on the focal spot of the lens. This is enough energy to burn a piece of paper.

The total power in the beam is the integral of the irradiance over the transverse profile of the beam

$$P = \int I \, dA. \tag{5.10}$$

This expression has already been discussed in Sec. 2.4 for the case of a gaussian beam.

From the quantal point of view, light is made of packets of energy

$$E_{\rm ph} = hf = \frac{hc}{\lambda}. \tag{5.11}$$

It is convenient to use the result $hc = 1240$ eV-nm. It let us calculate the energy of photons. For example, the energy of a photon with $\lambda = 500$ nm is $E_{\rm ph} = 2.48$ eV.

The number of photons of energy E traveling per unit time in a beam of power P is

$$N = \frac{P}{E_{\rm ph}}. \tag{5.12}$$

A 1 mW beam of photons of wavelength 500 nm carries $N = 2.5 \times 10^{15}$ s^{-1}.

Exercise 12 How many photons per second are emitted by a green laser pointer (5 mW, 532 nm)?

CCD cameras and solar cells take the energy of individual photons to release electrons via the photoelectric effect. In the case of the CCD camera, the photoelectrons go to define an image, and in the case of a solar cell they go on to power an electrical circuit. When we make the image of a distant galaxy, we gather the energy of photons produced in those remote locations, and which traveled millions if not billions of light years to reach us. Figure 5.2 shows the image of quazar 3C454.3, which is about 14 billion light years away–almost the age of the universe! This quazar was imaged at Colgate when it had an outburst in 2005, displaying 12 magnitude. The photon flux that we get from it on Earth is 1×10^5 photons/s-m^2.

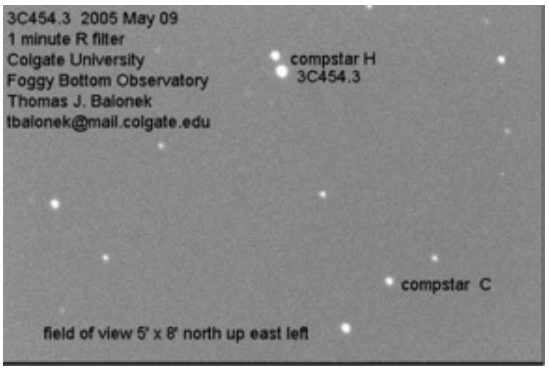

Figure 5.2: Image of quazar 3C454.3 taken at Foggy Bottom Observatory.

5.2 Linear Momentum

If all the energy of the electromagnetic field of a beam with power P is absorbed by an object, then the object experiences a force

$$F = \frac{P}{c}, \tag{5.13}$$

with P being defined in Eq. 5.10. The field thus exerts a radiation pressure on the object. Since the energy per unit time per unit area is S, then the radiation pressure is given by

$$P_{\mathbf{rad}} = \frac{S}{c}. \tag{5.14}$$

Thus, the light can exert a force on the object The momentum associated to the electromagnetic field is

$$p = \frac{u}{c} = \frac{S}{c^2}. \tag{5.15}$$

The momentum vector can then be defined as

$$\mathbf{p} = \epsilon_0 \mathbf{E} \times \mathbf{B} = \frac{\mathbf{S}}{c^2}. \tag{5.16}$$

The momentum associated to light is very small to make impact on macroscopic objects. However, microscopic objects and atoms are affected by radiation forces. It is convenient to define radiation dynamics in terms of photons. The momentum of a photon, defined by Einstein is given by

$$p_{\mathbf{ph}} = \frac{E_{\mathbf{ph}}}{c} = \frac{h}{\lambda}. \tag{5.17}$$

The momentum of a single photon is a very small amount. For example, the momentum of a 500-nm photon is 1.3×10^{-27} kg m s^{-1}. A sodium atom traveling in a room-temperature vapor has a momentum $p_{Na} = 2\times10^{-23}$ kg m s^{-1}. It would require a Na atom to absorb about 2×10^4 photons tuned to the D-line ($\lambda = 589$ nm) to slow it down. This is the basis of laser cooling of atoms. In the cooling process a beam of atoms is slowed down by absorption of photons traveling in the opposite direction in which they are going. Since re-emission goes in any direction, the Na atoms is effectively slowed down by consecutive absorptions followed by re-emission. This is the first step in a laboratory technique to slow and trap atoms to very low temperatures. Figure 5.3 shows a cloud of trapped Na atoms after being slowed down. The

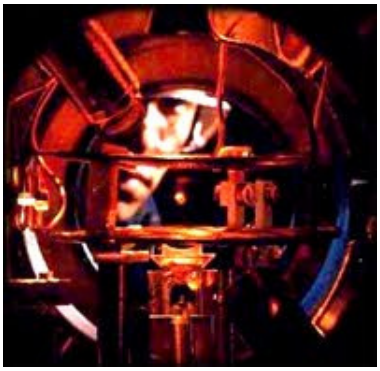

Figure 5.3: Photo of a Na cloud trapped at a temperature of 1 mK inside a vacuum chamber. Credit: Kris Helmerson, NIST Atomic Physics Group.

temperature of the cloud is 1 mK, which translates into atomic momenta of 4×10^{-26} kg m s^{-1}. If the trap is turned off it can easily be pushed away by a light beam.

Let us consider now macroscopic objects. If the object is submerged on a medium of index of refraction n_m then the radiation force of a beam of light carrying N photons per second is then

$$F_N = N n_m p_{\mathbf{ph}}. \tag{5.18}$$

For example, a 1-mW beam of 500-nm light, such as that of a laser pointer, exerts a force of 3.3 pN on an opaque object. Notice, however, that this is *larger* than the weight of common microscopic objects. Consider a model object like a microscopic cube of side $d = 50$ μm and density $\rho = 10^3$ kg/m^3. Its mass is 125 pg and its weight is 1.2 pN. If the The light forces on this object can vary depending on the reflecting properties of the cube. This is shown pictorically in Fig. 5.4. If the cube is fully absorbent the force is F_N. If it is fully reflective the force is $2F_N$. This is because the light gets a momentum change that is twice its incident momentum (i.e., $p_f - p_i = -2p_i$). If the cube is transparent then, only a fraction of the light gets

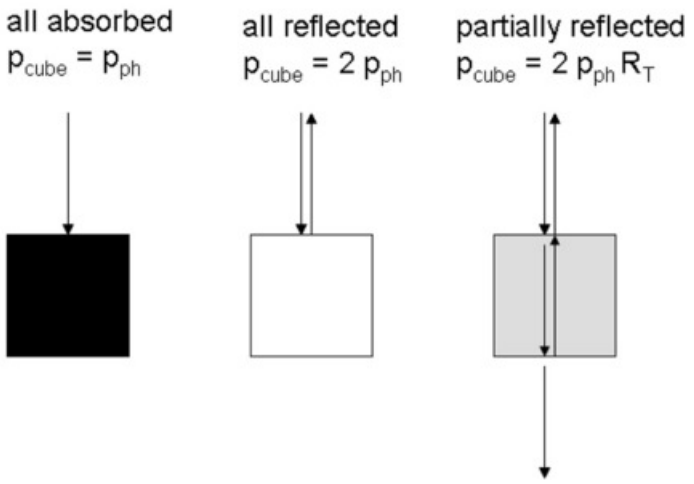

Figure 5.4: Possible situations when light is incident on a cube: the cube absorbs all the light (a), the cube reflects all of the light (b), and the cube reflects a partial amount of the light (c).

reflected. For normal incidence the reflection coefficient is $R = (n_m - n_c)^2/(n_m + n_c)^2$, where n_c is the index of refraction of the cube. For example, $R = 0.04$ for light going from air ($n_m = 1$) to glass ($n_c = 1.5$) and $R = 0.004$ for light going from water ($n_m = 1.33$) to glass. Thus the force from the first reflection is $2F_N R$. There are more forces: the force from the second reflection involves a transmission into the cube ($T = 1 - R$), a reflection at the bottom surface and a transmission out of the cube at the top surface. The force will be $2F_N TRT$. The next term would involve now two transmissions and three reflections, with a force $2F_N T^2 N^3$. The exact amount is an infinite series:

$$F_T = 2F_N R_T, \tag{5.19}$$

with

$$R_T = R + T^2 R \sum_{i=1}^{\infty} R^{2i}. \tag{5.20}$$

The infinite series $\sum_i x^2$ converges to $1/(1-x)$ when $x < 1$. In our case $x = R^2$. Therefore

$$R_T = R\left(1 + \frac{T^2}{1 - R^2}\right). \tag{5.21}$$

For a glass cube in air $R_T = 0.077$, and for the cube in water it is $R_T = 0.0072$.

5.2.1 Optical Tweezers

For example, a polystyrene microsphere with a diameter $d = 5$ μm has a mass of about 69 pg and a weight of about 0.67 pN. The effect of weight is further minimized if the sphere is submerged in water, where the buoyancy force is 0.64 pN. These forces scale as d^3.

Consider photons incident on a polystyrene sphere, as shown in Fig. 5.5. A fraction

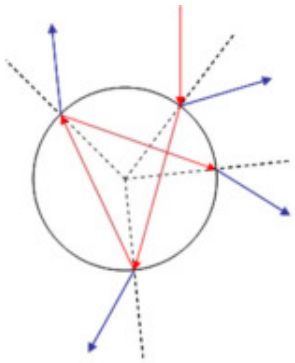

Figure 5.5: Trajectory of a light ray through a sphere.

of the photons get reflected at the first surface. Photons going in such a direction get a momentum kick by the sphere equal to the difference between the two momenta. By conservation of momentum the sphere gets an equal and opposite momentum kick. The same occurs with the photons exiting the sphere from the inside. If the sphere is uniformly illuminated it can be shown that the total force acting on the sphere is 0.4 F_N.

If instead of sending a light beam uniformly to a sphere we focus it we get a very interesting effect: optical forces work to create a position where the sum of forces on the sphere is zero, and when displaced from that position a restoring force appears. The ray-diagram view of this situation is shown in Fig. 5.6. The net effect is to trap the sphere. The trapping force is proportional to F_N. The maximum trapping force on spherical object can be found to be given by [1]

$$F_{\text{trap}} = \frac{Q n_m P}{c}, \tag{5.22}$$

where Q is a constant that depends on the geometry. In a typical situation it ranges betwen 0.01 and 0.5. Figure 5.7 shows an example of transverse (top row) and longitudinal trapping. In the top row one can see the sphere labeled by an arrow in frame

[1] A. Ashkin, "Forces of a Single Beam Gradient Laser Trap on a Dielectric Sphere in the Ray Optics Regime," Biophysical Journal **61**, 569-582 (1992)

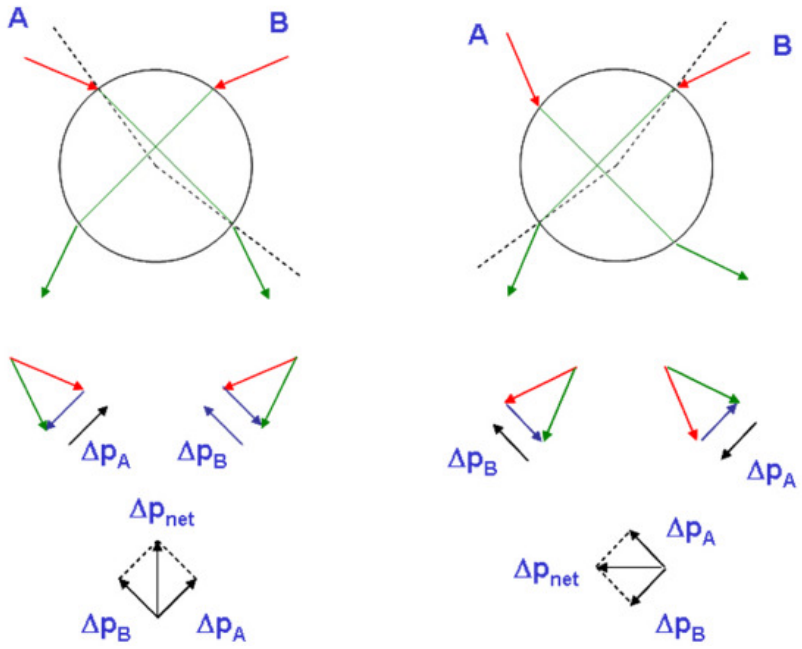

Figure 5.6: Trajectory of a light rays in an optical tweezer.

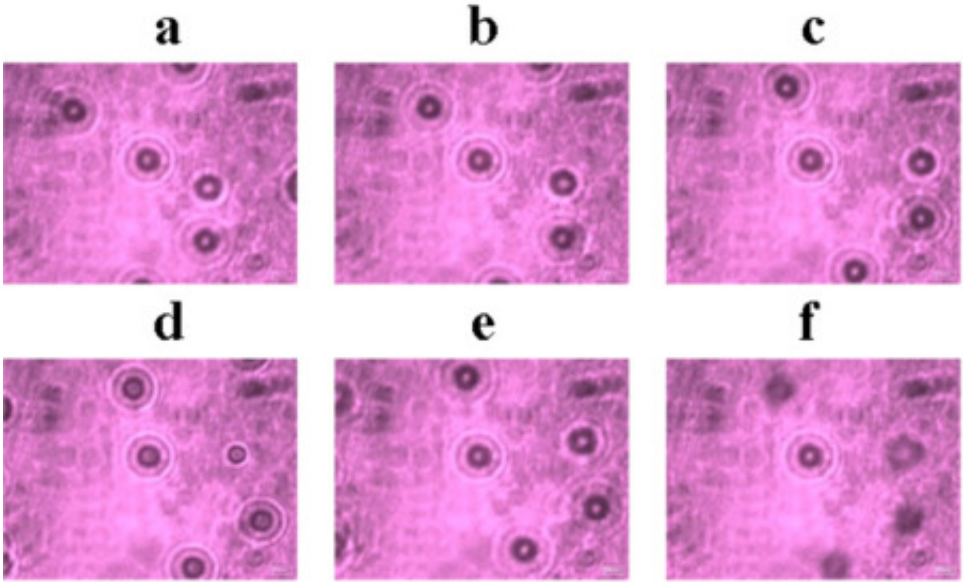

Figure 5.7: Images of a sphere trapped on a microscopic slide in an aqueous solution. Frames (a)-(c) show transverse trapping and frames (d)-(f) show longitudinal traping.

(a) at a fixed position relative to the background spheres. In this situation the microscopic slide was moved to the right, showing transverse trapping. These pictures were taken here at Colgate. In frames (d)-(f) of Fig. 5.7 the microscope was moved up and down, along the vertical direction of the trapping beam. As the microscope slide was moved vertically the spheres in the background got out of focus bu the trapped sphere stayed in focus. The trapping force in this longitudinal direction is much smaller.

One could measure this force using the drag force due to viscosity. For spherical objects it is given by

$$F_D = 6\pi\eta a v, \tag{5.23}$$

where η is the viscosity ($\eta_{\text{water}} = 10^{-3}$ Pl), $a = d/2$ is the radius of the sphere and v is the velocity of the sphere. For a sphere with $d = 5$ μm moving at a velocity $v = 5\mu$m/s the drag force is 0.24 pN. That is, it is also of the same order of magnitude as the other forces. We were able to move the sphere trapped for background sphere speeds of up to 60 μm/s. This translates into a drag force, and consequently maximum trapping force, of 3 pN.

Exercise 13 The maximum speed with which we could pull a 10-μ m sphere is 100 μm/s. What is the trapping force?

5.3 Angular Momentum

Light can also carry angular momentum. There are two distinct types of angular momentum. One is called "spin" angular momentum, and is due to the polarization of the light. The other type of angular momentum is due to dislocations in the wavefront of the light wave. Below we will discuss these two types of angular momentum.

Angular momentum density $\mathbf{j}$ of a light wave is defined in the same way as for material objects

$$\mathbf{j} = \mathbf{r} \times \mathbf{p}. \tag{5.24}$$

If we replace Eq. 5.16 for the momentum density of the field we have

$$\mathbf{j} = \mathbf{r} \times \mathbf{p} = \epsilon_0 \mathbf{r} \times (\mathbf{E} \times \mathbf{B}) \tag{5.25}$$

or

$$\mathbf{j} = \frac{\epsilon_0}{c^2} \mathbf{r} \times \mathbf{S}. \tag{5.26}$$

Notice something peculiar. If the light beam comes in the form of an infinite plane wave there is no angular momentum. This is because for a plane wave $\mathbf{S}$ is constant and parallel to the propagation direction at *all points* on the plane. Thus we need a beam of light for carrying angular momentum.

5.3.1 Polarization and Spin Angular Momentum

As seen before, light can be in a variety of polarization states. Circular polarization states are eigenstates of angular momentum. The electric field of a circularly polarized electromagnetic wave propagating along the z-axis can be represented as

$$\mathbf{E} = \frac{E_0}{\sqrt{2}}(\mathbf{i}\cos(kz - \omega t) \pm \mathbf{j}\sin(kz - \omega t)), \tag{5.27}$$

where the positive sign represents the state of right circular polarization, and the negative sign represents left circular polarization.

In this state the direction of the electric field of the light changes as the wave propagates. For example, if we were to freeze in time a right circularly polarized wave, the electric field direction would rotate counter-clockwise along the direction of propagation. This is seen in Fig. 5.8a. Another way to view this polarization state

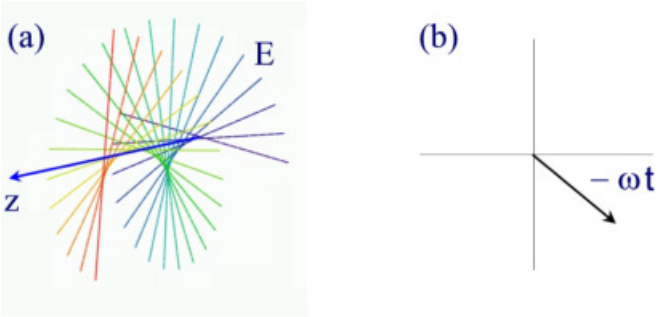

Figure 5.8: Representations of the electric field of a right circularly polarized wave: (a) as a function of the propagation direction at a given instant, and (b) as a function of time on a fixed point in space.

is by looking at the electric field as a function of time at a fixed point in space. If for example we set $z = 0$ in Eq. 5.27 we see that it describes an electric field that rotates clockwise as a function of time, as shown in Fig. 5.8. We are not going to derive an expression for the angular momentum of the light. The result is that the z component of the angular momentum of a beam of circularly polarized light is

$$J_z = \sigma\frac{P}{\omega}, \tag{5.28}$$

where P is, as before, the power of the beam. The quantity σ represents the helicity of the light, with $\sigma = -1$ for right circular polarization and $\sigma = +1$ for left circular polarization. For linearly polarized light $\sigma = 0$, while $0 < |\sigma| < 1$ for states of elliptical

polarization. If we replace P with $N\hbar\omega$, with N being the number of photons in the beam we get that the angular momentum per photon is

$$\frac{J_z}{N} = \sigma\hbar. \tag{5.29}$$

That is, each photon in a circularly polarized state carries $\hbar$ units of angular momentum.

Birefringent materials can insert phases between the components of the electric field parallel and perpendicular to the symmetry axis of the material. A quarter wave plate inserts a phase of 90° while a half-wave plate inserts a phase of 180°. A quarter-wave plate inserted in the path of a circularly polarized beam changes the polarization to linear. The converse is true if the quarter-wave plate is aligned properly. A half-wave plate changes the handedness of the circular polarization. Thus one can see waveplates as devices that exchange angular momentum with the light. In general, birefringent material in the path will exchange angular momentum with the light in some degree that depends on specific details of the material and the polarization state of the light.

One can observe this exchange of orbital angular momentum in an optical tweezer. By putting birefringent crystals in an aqueous sample on a microscope slide one can observe the rotation of the crystals by the angular momentum exchange with a circularly polarized trapping beam.

5.3.2 Orbital Angular Momentum

As discussed in a previous section, the complex amplitude of the field in Laguerre Gauss beams can have a phase term that depends on the transverse angular coordinate θ:

$$\mathcal{E} \propto e^{i\ell\theta}, \tag{5.30}$$

where ℓ is the phase winding number. As a consequence the wavefront consists of intertwined helices. In a wave that propagates in free space the direction of energy flow is perpendicular to the wavefront. In the case of a beam with a helical wavefront the linear momentum, which is perpendicular to the wavefront, has an axial component. If you imagine the circular ramp in a car garage, the normal to the pavement is not vertical: it is tilted toward points lower in the ramp. Thus, the linear momentum in a helical wavefront has a component along the propagation direction p_z, a component along the radial direction if the beam is expanding p_r, and a component along the *azimuthal* direction p_ϕ due to the tilted helix. Thus, the linear momentum vector in cylindrical coordinates is $\mathbf{p} = (p_r, p_\phi, p_z)$, as can be appreciated in Fig. 5.9. If we calculate the angular momentum relative to the axis of the beam we get that the

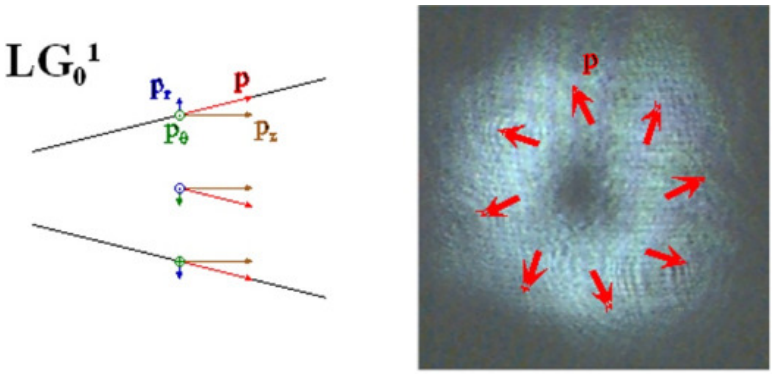

Figure 5.9: Directions of the linear momentum of the light for a Laguerre-Gauss beam with $\ell = 1$.

angular momentum has a non-zero z component:

$$\mathbf{j} = \mathbf{r} \times \mathbf{p} = r p_\phi \mathbf{k}. \tag{5.31}$$

The analytical evaluation of the z-component angular momentum density of a Laguerre-Gauss beam yields

$$j_z = \epsilon_0 \omega \ell |\mathcal{E}_{p\ell}(r, \phi, z)|^2. \tag{5.32}$$

The evaluation of this result involves getting the p_ϕ in terms of the field amplitude of the beam. It is an evaluation that is beyond the scope of this discussion. As can be seen from Eq. 5.32, the angular momentum density depends on the field amplitude. That is, the angular momentum is in the field that surrounds the beam axis, which contains an *optical vortex*. The total angular momentum of the beam can be calculated by integration of the angular momentum density over the transverse profile of the beam. The result is surprisingly simple:

$$J_z = \ell \frac{P}{\omega}, \tag{5.33}$$

where P is the power of the beam. If we use $P = N\hbar\omega$, with N being the number of photons in the beam. Thus the angular momentum of the beam per unit photon is:

$$\frac{J_z}{N} = \ell\hbar. \tag{5.34}$$

If we compare this result with the one of Eq. 5.29 we arrive at a fundamental result: the angular momentum per photon in a beam in a Laguerre-Gauss beam that is circularly polarized is $(\ell + \sigma)\hbar$. We note the temptation to think that photons are in different parts of the beam. That is incorrect. All photons in the beam are in the entire mode. If we restrict the beam by an aperture then we would have to recalculate the angular momentum of each photon going through the entire aperture.

5.3.3 Rotation in Optical Tweezers

If we send a beam carrying orbital angular momentum to an absorptive particle this particle will rotate. Figure 5.10 shows the rotation of a 10-μm particle that absorbs part of the light incident on it, which carries orbital angular momentum. The irregularities in the particle allow us to see its rotation.

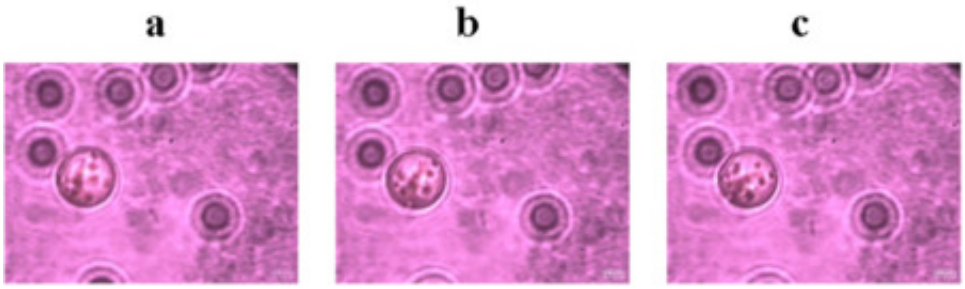

Figure 5.10: Images of a sphere trapped on a microscopic slide in an aqueous solution rotating by the action of orbital angular momentum.

The optical torque on an absorptive particle is

$$\tau = \frac{k\ell P}{\omega}, \tag{5.35}$$

where k is the fraction of power that is absorbed. As can be seen the torque depends on ℓ. The rotational drag torque on a sphere of radius R due to a fluid of viscosity η is

$$\tau_D = 8\pi\eta R^3\Omega, \tag{5.36}$$

where Ω is the frequency of rotation of the sphere. Thus one can use the orbital angular momentum of the light to do microrheology.

5.4 Problems

Problem 13 Suppose that we have a $d = 50$-μm glass cube with a mass density $\rho = 1.2 \cdot 10^3$ kg/m^3.

1. What is its weight?

2. If we send a beam of light upwards toward the cube. How much irradiance is needed to balance the cube against its weight?

3. How much irradiance would be needed to balance it in air if the cube is fully absorptive?

4. Now consider the cube to be a 50-50 beam splitter of the same size ($d = 50$ μm), such that when illuminated from below it transmits half of the light and reflects half of the light.

   (a) What irradiance is needed to keep it from falling down?

   (b) What is the total force acting on the cube? Make a diagram and explain your reasoning.

Problem 14 Consider Fig. 5.7. The diameter of the sphere is 5 μm. In frames (a), (b) and (c) it is being dragged at constant speed through the liquid. The time between frames is 1 s.

1. Estimate the speed of the sphere.

2. Find the force exerted by the light.

3. If this force is the maximum exerted by the trap, how much power is delivered onto the sphere?

Problem 15 Consider Fig. 5.10. The diameter of the sphere is 10 μm. The average time between frames is 5 s.

1. Estimate the angular frequency of rotation of the sphere in rad/s.

2. What is the torque exerted by the light on the sphere?

3. If the total power incident on the sphere is 50 mW, what fraction of the light was absorbed by the sphere?